FABRICATION AND CHARACTERIZATION OF GRANULAR MAGNETIC GOLD NANOPARTICLES

by

RISHI WADHWA

Presented to the Faculty of the Graduate School of

The University of Texas at Arlington in Partial Fulfillment

of the Requirements

for the Degree of

MASTER OF SCIENCE IN MATERIAL SCIENCE AND ENGINERING

THE UNIVERSITY OF TEXAS AT ARLINGTON

December 2008

ACKNOWLEDGMENTS

The author would like to express his sincere gratitude to Dr. Yaowu Hao, his research advisor, for his excellent guidance and constant encouragement throughout the research work. He would like to thank Dr. Ali R. Koymen and Dr. Efstathios I. Meletis for their participation as his committee members.

He also wants to thank Punnapob Punnakitikashem, Kevin and Mark for their enduring help in completing the research work for the thesis. He also wants to thank the other lab mates Grace, Chivarat and Orathai for their support and help. Further the author would like to mention about the various UTA labs that helped in completing the research work, Nanotechnology Research and Training Facility along with their staff for their excellent trainings on equipments.

The author also wishes to express his thanks to his friends Gitima Sharma, Vikram Singh, Sunil Singh Gusain, Pruthul Desai and Gaurav Arya for their moral support and help. He also expresses his sincere appreciation to his parents, sister and brother in law for their persistent support and encouragement.

December 10, 2008

ABSTRACT

FABRICATION AND CHARACTERIZATION OF GRANULAR MAGNETIC GOLD NANOPARTICLES

Rishi Wadhwa, M.S.

The University of Texas at Arlington, 2008

Supervising Professor: Yaowu Hao

In recent years, gold and magnetic nanoparticles have showed great potential in biomedical applications. Magnetic nanoparticles can be used in both *in vivo* and *in vitro* applications such as drug and gene delivery, hyperthermia treatment of cancer, magnetic resonance imaging (MRI) contrast enhancement, cell labeling, and bioseparation. Due to the surface plasmon resonance (SPR) effect, gold nanoparticles strongly absorb and scatter visible and infrared light in resonance with SPR, which is the reason why different sizes and shapes of Au nanoparticles exhibit different colors. They have been exploited for bioimaging and photothermal therapy applications.

In this thesis, we are investigating a new type of nanoparticles, granular magnetic Au particles. The particle size ranges from 10nm to 200nm. These nanoparticles have the potential to combine the properties of both gold nanoparticle and the magnetic nanoparticle into one nanoentity to provide multifunctionality. For

example, magnetic Au nanoparticles can be concentrated to a tumor sites by an external magnetic field gradient and photothermal therapy can be performed to locally kill tumor cells. A scalable, straight forward and inexpensive process using electrochemical deposition is being developed to produce these multifunctional nanoparticles. The process involves multilayers of gold and cobalt using a one-bath electrolyte containing both gold and cobalt in a porous polycarbonate membrane. By varying the deposition potential, gold and cobalt can be selectively deposited. The deposition time of both gold and cobalt were varied to manipulate the thickness to achieve the superparamagnetic property. Before depositing the multilayers, gold, cobalt or copper was used as a sacrificial layer for releasing the nanoparticles into solution. The magnetic properties were measured using alternating gradient magnetometer (AGM) and vibrating sample magnetometer (VSM). The structural properties were characterized through scanning electron microscopy (SEM), X-ray diffraction and transmission electron microscopy (TEM).

TABLE OF CONTENTS

LIST OF ILLUSTRATIONS

Figure Page

LIST OF TABLES

CHAPTER I

INTRODUCTION

Nanotechnology has marked the dawn of a new era with respect to unique material properties and has enthralled the world by its amazing applications particularly in the field of electronics and biotechnology. Nanotechnology today holds answers for how we can increase the capabilities of electronic devices while also reduce their weight and power consumption. In the biomedical field, it has allowed scientists, engineers and physicians to work at the cellular and molecular levels. This has led to major advances in the field of life sciences and healthcare. Though the commercial applications of nanoparticles in biomedicine are not very common at the present time, their excellent properties in comparison to their counterpart bulk materials provide a very promising future in this field [1, 6, 27].

As the size of the particle changes some radical transformation can be observed in their properties and hence some very useful results can be obtained particularly for bioapplications. This is because the size of nanoparticles employed is comparable to a lot of biological entities like cells (10-100micron), a virus (20-450nm), a protein (5-50nm) and a gene (2nm wide and 10-100nm long)[1,2, 25].

Various kinds of nanoparticles like magnetic nanoparticles, gold nanoparticles as well as their combination are utilized in the biomedical field. Biomedical applications can be broadly classified according to their application inside the body (*in vivo*) or outside the body (*in vitro*). Examples of in vivo applications include hyperthermia, drug-targeting and magnetic resonance imaging (MRI). Some examples of *in vitro* applications include cell separation and labeling. However, different biomedical applications impose strict requirements on particle's physical, chemical and structural properties including chemical composition, granulometric uniformity,

crystal structure, magnetic behavior, surface structure, adsorption property, solubility and low toxicity [1,2,6].

For magnetic nanoparticles for biomedical applications, superparamagnetic nanoparticles (zero remanance along with rapidly changing magnetic states) are desired. This is because they do not retain their magnetization even after removing the applied magnetic field [1, 2, 6]. For *in vivo* applications, the particle size should be small enough to remain in circulation after injection and to pass through the capillary systems of organs and tissues [6, 22]. They should have good surface characteristics and be biocompatible. In addition, they must have a high magnetization to generate enough force or signal [23]. For *in-vitro* applications such as cell separation, the magnetic particles should be stable and possess high magnetic moment [28, 29].

Gold nanoparticles are another type of nanoparticles that have immense potential in biomedical field. They are chemically stable, non toxic and can be tuned to various sizes and shapes. Gold nanoparticles are also functionalizable for biomolecule attachment. One of the most important characteristic of gold nanoparticles is a phenomenon called Surface Plasmon Resonance (SPR). According to SPR, when light is shone on gold nanoparticles of different sizes, shapes or composition, they appear of different colors. Because of this property, gold nanoparticles are commercially used in rapid testing arrays, like pregnancy tests and other bio-molecule detectors [12, 14, 16, 17]. Such applications are based on the fact that color of the colloid depends on particle size, shape, refractive index of the surrounding media and separation between the particles. A change in any of these parameters will result in a prominent shift in the SPR absorption peak. [14, 16].

A combination of these two nanoparticles results in a special nanoparticle which have properties of both gold as well as the magnetic nanoparticle. These magnetic gold nanoparticles can be manipulated by a magnetic field gradient together with exhibiting Surface

plasmon resonance. Because of these properties, they can be used in various bioapplications. This is just the motivation of this thesis.

CHAPTER 2

BACKGROUND INFORMATION AND LITERATURE REVIEW

2.1 Introduction to magnetism in small magnetic structures

2.1.1 Basics of magnetism

If a magnetic material is placed in a magnetic field of strength H, the individual atomic moments contribute to its overall response; the magnetic induction is given by:

$$B=\mu_o (H+M)$$

where μ_o is the permeability of free space, and the magnetization M is the magnetic moment per unit volume. All materials are magnetic to some extent, with their response depending upon their atomic structure and temperature. They can be classified in terms of their volumetric susceptibility χ, where

$$M= \chi H$$

describes the magnetization induced in a material by H.

Classes of Magnetic materials

The best way to explain different types of magnetic material is to understand how material responds to magnetic field. The magnetic behavior of materials can be classified into the following three groups-

Diamagnetism

Diamagnetism is a fundamental property of all matter and is usually very weak. It is due to the non-cooperative behavior of orbiting electrons when exposed to an external magnetic field. Diamagnetic substances are composed of atoms which have no net magnetic moments (i.e. all the orbital shells are filled and there are no unpaired electrons). However

when exposed to a field, a negative magnetization is produced and the susceptibility is negative. If we plot M vs. H, we see

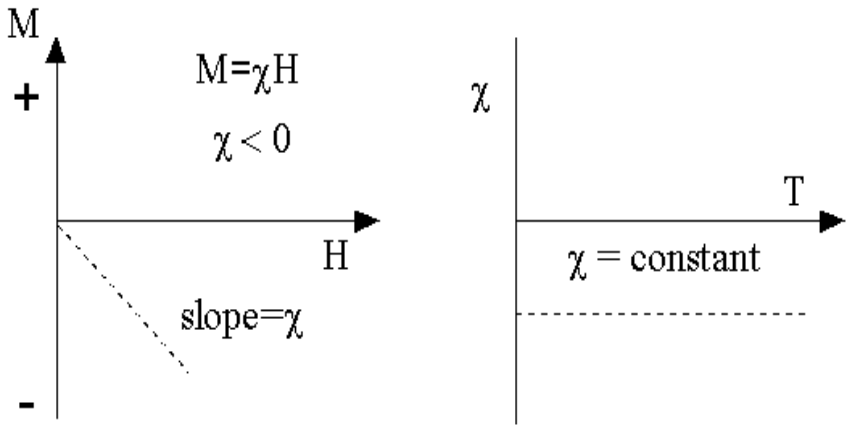

Figure 2.1 Diamagnetism

Paramagnetism

In paramagnetic materials, some of the atoms or ions in the material have a net magnetic moment due to unpaired electrons in partially filled orbitals. However, the individual moments do not interact magnetically, and like diamagnetism, the magnetization is zero when the field is removed. In the presence of a field, there is now a partial alignment of atomic magnetic moments in the direction of field, resulting in a net positive magnetization and positive susceptibility.

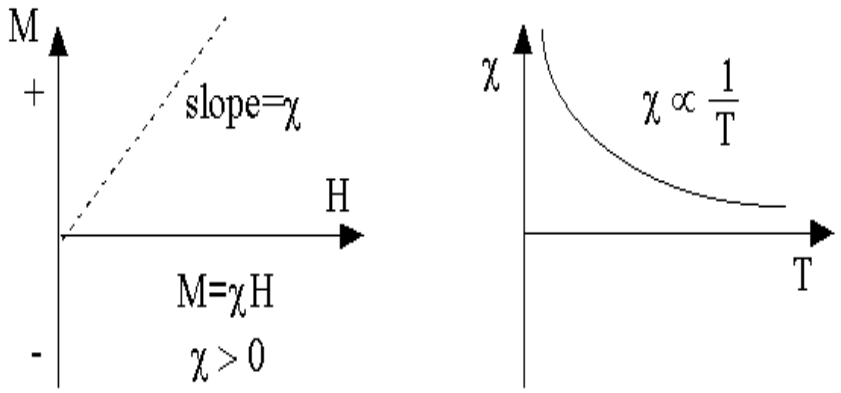

Figure 2.2 Paramagnetism

Ferromagnetism

Unlike paramagnetic materials, the atomic moments in these materials exhibit very strong interactions. These interactions are produced by electronic exchange forces and result in a parallel or antiparallel alignment of atomic moments. Exchange forces are very large, equivalent to a field on the order of 1000 Tesla, or approximately a 100 million times the strength of the earth's field. Ferromagnetic materials exhibit parallel alignment of moments resulting in large net magnetization even in the absence of a magnetic field. The elements Fe, Ni, and Co and many of their alloys are typical ferromagnetic materials. There are two distinct characteristics of ferromagnetic materials: Spontaneous magnetization and the existence of magnetic ordering temperature.

Various energy terms

Magnetic phenomena in small magnetic structures can be understood by considering that the state of magnetization is determined by minimizing the combination of 4 energy terms: Zeeman energy, Exchange energy, Magnetocrystalline energy and Magnetostatic energy.

Zeeman energy

Zeeman energy is the energy of magnetization in an externally applied magnetic field. It is often referred to as magnetic potential energy. Zeeman energy is always minimized when the magnetization is aligned with the external magnetic field. Zeeman energy is expressed as:

$$E_z = -M.H$$

where 'H' is the magnetic field applied and M is the moment.

Exchange energy

Exchange energy is a measure of the strength of the electrons spin exchange coupling. This energy term is responsible for the metals like iron, Cobalt and Nickel to be ferromagnetic. Exchange energy is lowest when atomic moments align themselves parallel to each other.

Magnetocrystalline anisotropy

Not only the atomic moments point to one direction but they point to a particular crystallographic orientation which is called easy axis. Anisotropy energy is the energy required to change the direction of atomic moments from easy axis to hard axis.

Anisotropy energy is defined as:

$$E = K\mathrm{Sin}^2\Theta$$

where K is the anisotropy constant.

Magnetostatic energy

A uniformly magnetized specimen has a large magnetostatic energy which is the result of presence of magnetic free poles at the surface of the specimen. These free poles generate a demagnetizing field. The high energetic cost of forming magnetostatic charges on the surface can often be reduced by introducing non-uniform magnetizations. This may increase the exchange energy, crystalline anisotropy energy and Zeeman energy, but the total

energy is lowered. This sometimes results in the formation of a structure within magnetic elements called domains.

Magnetic domains

In order to reduce the large magnetostatic energy, magnetic structures tend to form closed magnetization states. The formation of domains depends on the balance of exchange energy, anisotropy energy and magnetostatic energy. That is, the gain in reduction of magnetostatic energy has to be larger than the energy cost of the formation of a domain wall.

As seen in the figure 4.3, magnetostatic energy can be approximately halved if the magnetization splits into two domains magnetized in opposite direction. This brings (+) and (-) charges closer together thus decreasing the spatial extent of magnetic field. This subdivision into more and more domains cannot continue indefinitely because the transition region between domains (called domain wall) requires energy to be produced and maintained. Eventually an equilibrium number of domains will be reached for a given particle size. Domain walls are interfaces between regions in which the magnetization has different directions. Within the wall, the magnetization must change direction from that in one domain to that in another domain.

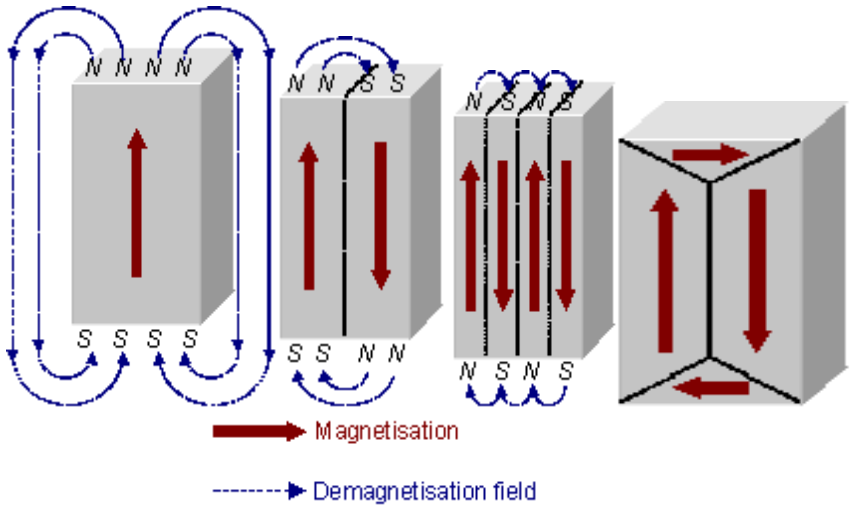

Figure 2.3 Magnetic domains

As the particle size keeps on decreasing, a critical size is reached when the particle can no longer accommodate a wall. At this point, a single domain is obtained. A single domain is uniformly magnetized to the saturation magnetization [2].

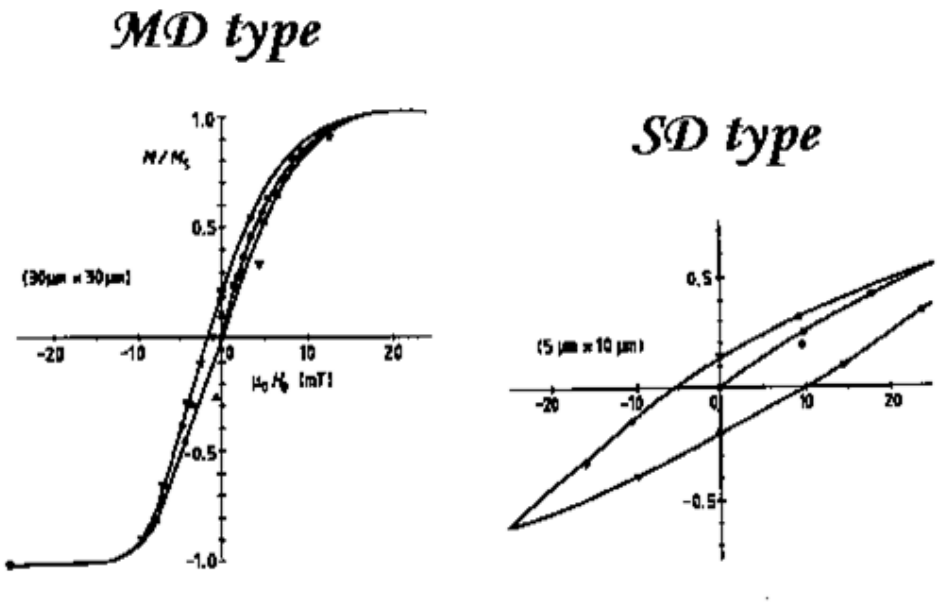

Figure 2.4 Hysteresis properties of single domain and multi domain particles

2.1.2 Superparamagnetism

As particle size continues to decrease within the single domain range, another threshold is reached, at which remanence and coercivity goes to zero. When this happens, the particle becomes superparamagnetic. A single domain particle of volume v has a uniform magnetization directed along the easy axis of magnetization. To change the direction of moment of a superparamagnetic particle from one direction to another an energy barrier must be crossed.

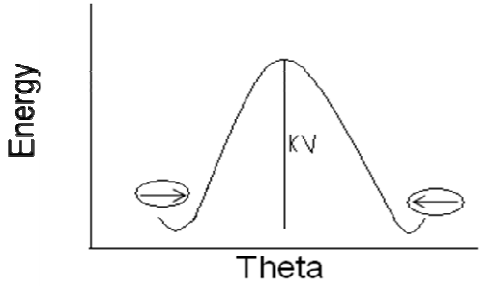

Figure 2.5 Superparamagnetism-Thermally activated switching of the net moment direction

The probability for a particle to overcome the energy barrier is given by the equation:

$$1/t = P = f\, e^{-KV/kT}$$

1/t is the probability whether the energy barrier will be crossed or not. 'P' is defined as the number of times the electron is able to change the direction successfully in one second. f is called frequency factor or thermal attempt frequency (10^9 sec^{-1}) and it is defined as the number of times the electron tries to switch from an easy axis to hard axis per second. For a magnetic particle its value is 10^9 times/second. K_u is anisotropy constant, V is the volume of the particle, k is Boltzmann constant and T is absolute temperature.

If 'v' is small enough or the temperature is high enough, KV is comparable to kT and hence thermal energy will be sufficient to overcome the anisotropy energy and cause a spontaneous reversal of magnetization [1, 2].

For superparamagnetic (SPM) particles, the net magnetic moment in zero field at T>0K, will average to zero. In an applied field however, there will be a net statistical alignment of magnetic moments. This is analogous to paramagnetism, except now the magnetic moment is not of a single atom, but of the entire particle. Hence the term superparamagnetism, which denotes a much higher susceptibility value than that for simple paramagnetism.

SPM particles exhibit no remanance or coercivity. The shape of the hysteresis loop is thus extremely thin. SPM particles show a very steep rise in magnetization with field and then a more gradual increase to saturation.

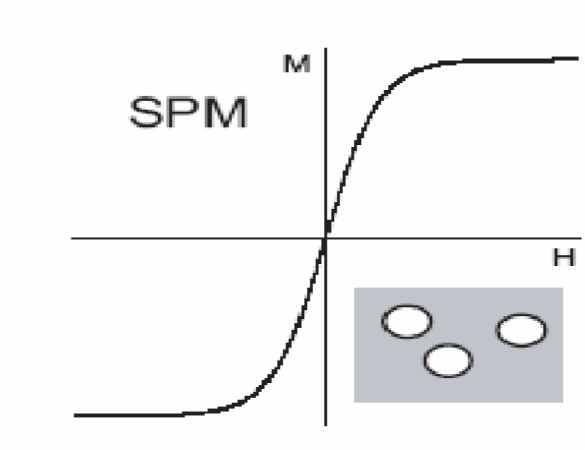

Figure 2.6 Superparamagnetic hysteresis properties

2.1.3 Literature review on synthesis of magnetic nanoparticles

The syntheses of magnetic nanoparticles for bioapplications are classified into two major categories-1) Composites containing nanoparticles dispersed in organic or inorganic matrixes. 2) Magnetic nanoparticles produced from solution techniques or aerosol/vapor phases.

Precipitation from solution

Many scientists explained the formation of uniform particles by homogeneous precipitation reactions. In these reactions, nucleation occurs when the concentration of constituent species reaches supersaturation. Then the nuclei grow uniformly by diffusion of solutes from the solution to their surface until the final size is obtained.

Microemulsions

This is a very simple and versatile method to prepare nanoparticles and is used in a lot of in vivo and in vitro applications. In this method, nanosized magnetic particles are prepared with their size ranging from 4-12nm using microemulsions. In this method fine micro-droplets of the aqueous phase are trapped within a group of surfactant molecules dispersed in a continuous oil phase. The microcavities stabilized by the surfactant molecules provide a confinement effect which limits particles nucleation, growth and agglomeration [1,2].

Polyols

Polyol technique is one of the most promising method used for the preparation of uniform nanoparticles. Fine metallic nanoparticles can be obtained by reduction of dissolved metallic salts and direct metal precipitation from a solution containing polyol. This method is used to prepare various magnetic particles such as Fe, Ni and Co [1, 19, 20].

Electrochemical methods

Electrochemical methods have also been used for the production of magnetic nanoparticles. An example is the electrochemical synthesis of Fe_2O_3 in an organic medium. The size is controlled by current density and the particles are stabilized as a colloidal suspension [1,21].

2.2 Introduction to optical properties of colloidal gold

Gold nanoparticles having appropriate size scale exhibit unique optical properties and are a lot of interest in biology and medicine. They have immense potential in applications like cancer diagnosis and therapy because of their surface plasmon resonance (SPR) enhanced light scattering and absorption. Molecular specific imaging and detection of cancer is possible by conjugating Au nanoparticles to ligands which are then targeted to cancer cells. Also they have the ability to convert the strongly absorbed light into localized heat. This property of Gold nanoparticles can be used in photothermal therapy of cancer [12, 13].

2.2.1 Surface plasmon resonance

Beautiful colors like red or purple can be generated on a piece of glass by adding gold to it. Faraday attributed this color to very finely divided colloidal gold or gold nanoparticles. He found out that as the size or shape of the nanoparticles changes, the observed color also changes. Many recent experiments have proven that the color change due to size is because of collective oscillation of the electrons in the conduction band, known as the surface plasmon oscillation. This oscillation frequency is usually in the visible region for noble metals like gold and silver giving rise to the strong surface plasmon resonance absorption. [13]

An important aspect of metal nanoparticles is that when they are enlarged their optical properties do not change that much. However when anisotropy is added to the nanoparticle, for example in case of the formation of nanorods, the optical properties change drastically. This can be observed in the following figure:

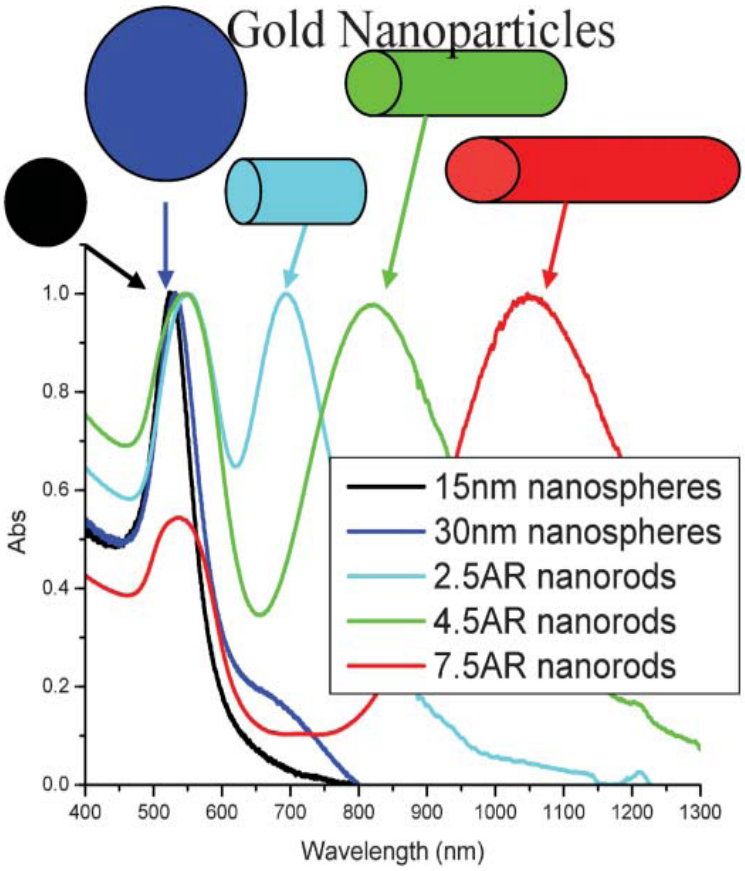

Figure 2.7 Variation of optical properties with size and shape of nanoparticles

The ‘d’ electrons in gold are free to travel through the material. The mean free path in gold is about 50nm. For a nanoparticle smaller than this size, no scattering is expected from the bulk and hence all interactions occur from the surface. If the wavelength of light is larger than the nanoparticle size it leads to standard resonance oscillations. Light in resonance with the surface plasmon oscillation causes free electrons in the metal to oscillate. As the light wave passes through the particle, the electron density in the particle is polarized to one surface and oscillates in resonance with the light’s frequency causing a standing oscillation as shown in the figure [13].

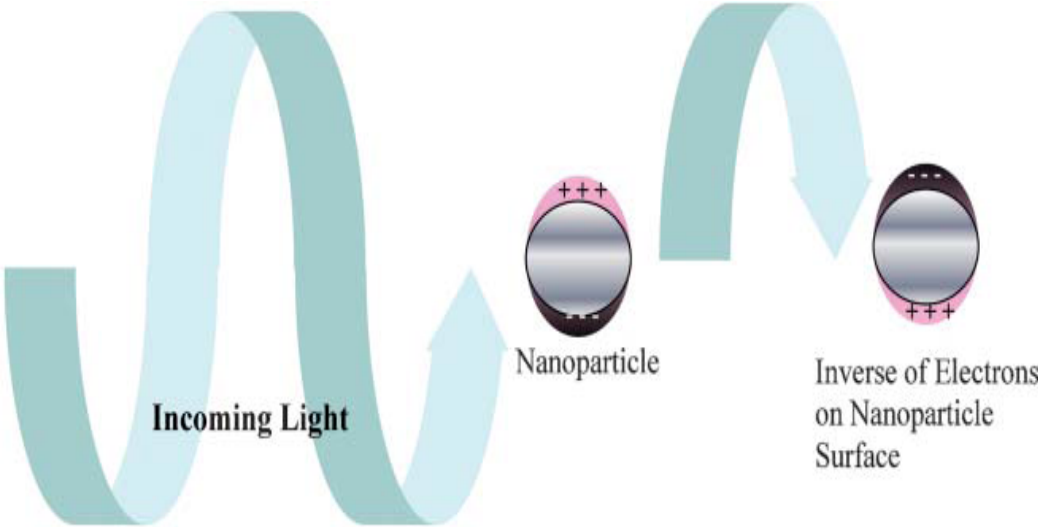

Figure 2.8 Surface plasmon resonance due to coherent interaction of the electrons in the conduction band with light.

The resonance condition is determined from absorption and scattering spectroscopy and is dependent on the shape, size and dielectric constants of both the gold nanoparticle and the surrounding material. Since it is a surface phenomenon it is referred to as the surface plasmon resonance. As the shape or size of the nanoparticle changes, the surface geometry changes causing a change in the oscillation frequency of the electrons, generating different cross-sections for the optical properties including absorption and scattering. [12, 13, 14, 18]

Many shapes of Gold nanoparticles have been synthesized out of which nanorods have attracted the most attention. This is because a lot of synthetic methods are available for their preparation in which high monodispersity and control over their aspect ratio (which is primarily responsible for the change in their optical properties) is possible. There are two types of plasmon resonances in nanorods; one due to the transverse oscillation of the electrons around 520nm wavelength for gold and other due to the longitudinal plasmon resonance at longer

wavelengths. The transverse surface plasmon resonance does not depend upon the aspect ratio while the longitudinal surface plasmon resonance increases with larger aspect ratio. [13]

2.2.2 Literature review on synthesis of gold nanoparticles

The two most common methods of fabrication of Gold nanoparticles are citrate reduction and The Burst-Schiffrin method.

Citrate reduction

Among the various conventional methods of synthesis of Au nanoparticles the method which is most commonly and widely used is the citrate reduction of $HAuCl_4$ in water. The size of the nanoparticles obtained through this method is about 20nm. To prepare controlled size of Au nanoparticles, the ratio between trisodium citrate to gold ratio (reducing agent/stabilizing agent) was varied. This method is also used often when a loose shell of ligands is required around the gold core [16, 17, 18].

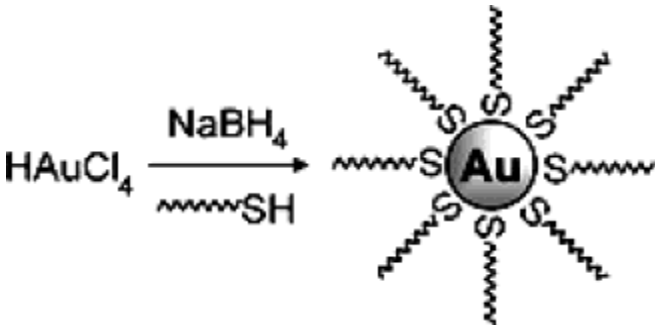

Figure 2.9 Formation of Au NPs coated with organic shells by reduction of Au compounds in the presence of thiols**.**

Another method of preparation of sodium 3-mercaptopropionate stabilized gold nanoparticles happens by simultaneous addition of citrate salt and an amphiphile surfactant. The size of the nanoparticles can be controlled by varying the stabilizer/gold ratio [16].

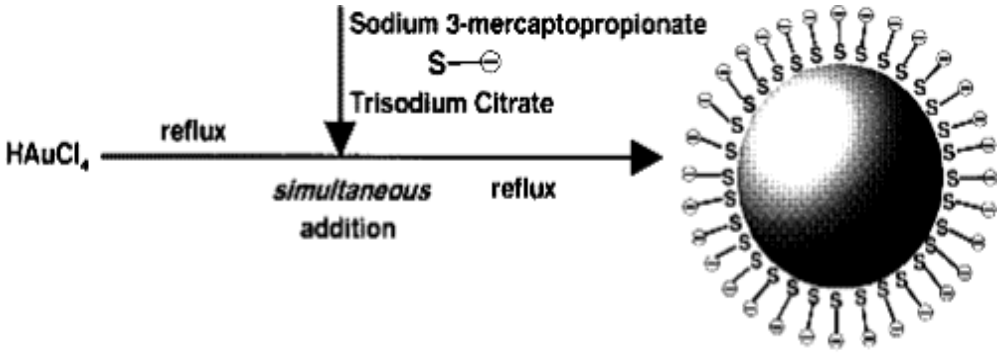

Figure 2.10 Preparation of stabilized gold nanoparticles

The Burst-Schiffrin Method: Two phase synthesis and stabilization by Thiols

The Burst-Schiffrin method is an easy synthetic process of developing thermally stable gold nanoparticles. The Au nanoparticles formed from this method are monodisperse in nature and of controlled size. They can be repeatedly isolated and redissolved in common organic solvents without irreversible aggregation or decomposition.

In this technique the thiol ligands is strongly bonded to gold. $AuCl_4$. $AuCl_4$ is transferred to toluene using tetraoctylammonium bromide as the phase transfer reagent and reduced by $NaBH_4$ in the presence of dodecanethiol. As soon as $NaBH_4$ is added the color changes from orange to deep brown within a few seconds. The following reaction takes place in forming the nanoparticles:

$$AuCl_4^- (aq) + N(C_8H_{17})_4^+ (C_6H_5Me) \rightarrow N(C_8H_{17})_4^+ AuCl_4^- (C_6H_5Me)$$

$$mAuCl_4^- (C_6H_5Me) + nC12H_{25}SH(C_6H_5Me) + 3_m e \rightarrow 4mCl_4^- (aq) + [Au_m (C_{12}H_{25}SH)n(C_6H_5Me)]$$

A higher abundance of small core sizes (< 2nm) is obtained by quenching the reaction immediately following reduction or by using sterically bulky ligands [16,17,18].

Preparation using methanol solution of gold ions

Another method which is very commonly used in the fabrication of gold nanoparticles is using methanol solution of gold ions. Very fine gold nanoparticles can be obtained by preparing methanol solution of gold ions. This solution is prepared by dissolving crystalline hydrogen tetrachloroaurate ($HAuCl_4 \cdot xH_2O$) in 25ml of Methanol. Then a solution of 150mg of Poly (N-vinyl-2 pyrrolidone) in 25ml of Methanol was added to the metal ion mixture. Also to reduce the metal ions, 6ml of an aqueous solution of $NaBH_4$ was added to the mixture dropwise at room temperature. After its addition a homogeneous colloidal dispersion of Gold nanoparticles was formed. By using this method, the size of gold nanoparticles increases if the concentration of gold ions in the reaction mixture increases and vice-versa. For example, the average particle size obtained varied from a few nanometers at 0.033mmol to approximately 12nm at 0.12mmol metal ion content in the reaction mixture [13, 14, 16, 18].

2.3 Core shell magnetic gold nanoparticles

In many areas of biological application, it is important to modify the surface properties because the magnetic nanoparticles should have the desired biocompatibility. There are many approaches for modifying the surface of the magnetic nanoparticles with materials such as polymers, oxides and metals. However, one of the most promising systems involves the usage of magnetic nanoparticle coated with gold shells [15]. The structure of the core shell magnetic nanoparticles is shown in the figure:

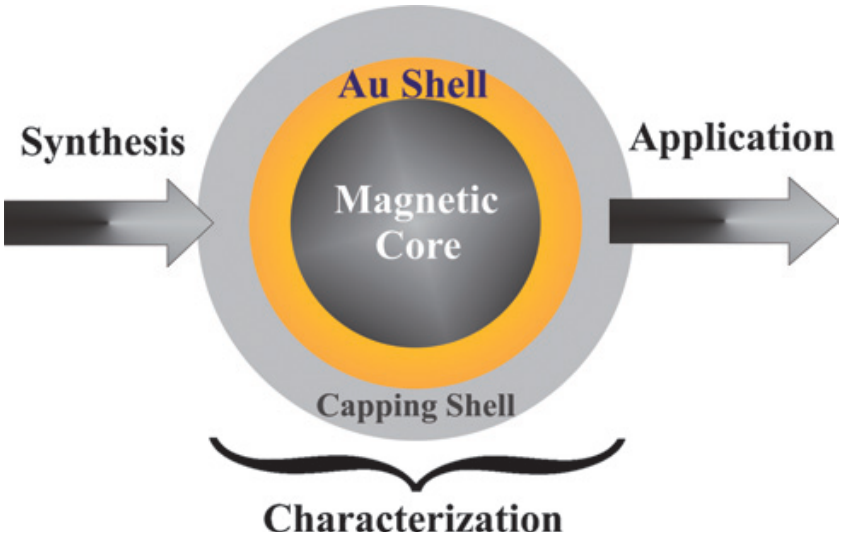

Figure 2.11 Magnetic core gold shell nanoparticles

Core-shell magnetic nanoparticles have wide range of applications including magnetic separation, tagging bifunctional molecules or antibodies which can then target different antigens [16]. Gold shell imparts the magnetic nanoparticles with many functional properties. Core-shell system enhances stabilization, has a biocompatible surface and exposes the surface with desired chemical, biological or catalytic interfacial activities [15, 17].

Synthesis of Core shell magnetic nanoparticles

There are a number of methods of fabrication through which these core shell magnetic gold nanoparticles can be synthesized. In the first method there is a sequential formation of the iron oxide core and gold shell. First the seeds of Fe_3O_4 are synthesized. After the formation of the Fe_3O_4 seeds of appropriate sizes, gold is deposited onto the surface of Fe_3O_4 by reduction of Au $(CH_3COO)_3$ using 1,2- hexadecanediol as a reducing agent. This reaction is carried out in the presence of capping agents at elevated temperature (180°C- 190°C). The reaction temperature controls the partial desorption of the capping layer from the core, the deposition of Au on the exposed Fe_3O_4 surface and the confinement of the Au shell surface by the capping

agent. These are all thermally activated processes and therefore temperature is a key factor in the formation of these nanoparticles. The resulting Fe_3O_4 nanoparticles can be separated from the uncoated Fe_3O_4 nanoparticles by centrifugation. With this method highly monodisperse Fe-oxide-Au nanoparticles have a core size ranging from 5 to 15nm with a shell thickness of 0.5-2nm. The thickness can be controlled by controlling the reaction time and concentration of Au [15, 17].

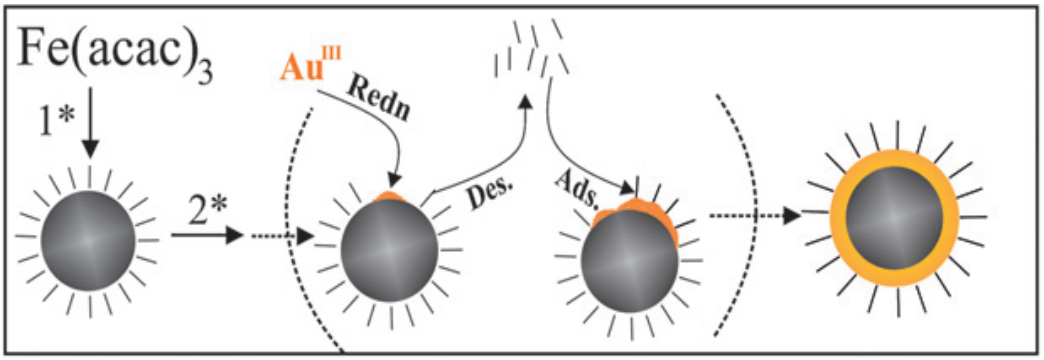

Figure 2.12 Sequential formation of magnetic core gold shell nanoparticles

In another method, iron-oxide nanoparticles and Au nanoparticles are mixed as precursors in a solution which is heated at high temperature. The principle behind fabricating the core shell type nanoparticles is that there is an interparticle coalescence of gold and magnetic nanoparticles [Fe_2O_3@Au] due to thermal activation if the temperature is increased. The fundamental basis for this stems from the decrease of melting point, especially the surface melting. Various other organic compounds are there in the solution to create the best processing environment for the stabilization of nanoparticles, including tetraoctylammonium bromide (TOABr) in the solution and capping materials such as alkanethiols for capping gold nanoparticles and oleic acid for capping Fe- oxide nanoparticles. Molecularly-capped iron oxide nanoparticles present in the solution create a unique thermal microenvironment for the

core@shell coalescence to produce monodisperse Fe-oxide@Au nanoparticles of controlled sizes [15, 17].

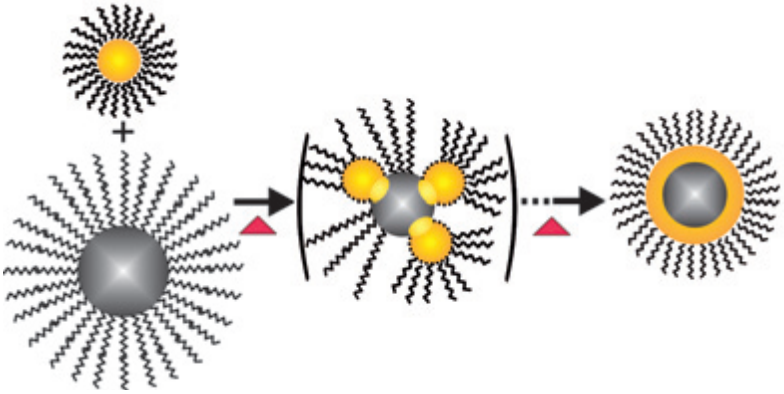

Figure 2.13 Synthesis of hetero-interparticle coalescence of Au and Fe_2O_3 nanoparticles

The gold shell thickness can be manipulated depending on the relative ratio of Au and Fe-oxide precursors. The rate of growth of Au and Fe-oxide@Au with single or multiple Fe-oxide cores nanoparticles is determined by a combination of the solution temperature, the composition and the capping structures.

However the core shell magnetic nanoparticles have a lot of drawbacks. First, their process of formation is very complicated. This is because before fabricating core shell magnetic nanoparticles, it is required to fabricate gold nanoparticles and magnetic nanoparticles separately and then combine them by homo-interparticle or hetero interparticle coalescence. Secondly, it is very difficult to control the thickness of gold and hence capping materials need to be used. The process has to be carried out at a higher temperature.

CHAPTER 3

FABRICATION AND CHARACTERIZATION METHODS

3.1 Template synthesis

This method is used for the fabrication of various micro and nanomaterials and involves the synthesis of a desired material within the pores of a nanoporous membrane. It is called template synthesis because the pores within these nanoporous membrane act as templates for the synthesis of nanostructures of the desired material. The membranes that are used have cylindrical pores of uniform diameter and hence nanocylinders of the desired material is grown in each of the pore [4]. Most of the research in template synthesis is done on two types of templates-1) Track etch polymeric membranes; 2) Porous alumina membranes

Both these membranes are used in fabricating various structures like nanodisks, nanorods and nanowires which are used in various electronic and biomedical applications. Electrochemical methods are very commonly used for developing these nanostructures [7, 11].

3.2 Electroplating principle

Electroplating is the process of using electrical current to reduce cations of a desired material from a solution and coat a conductive thin layer of a material such as metal.

When a metallic salt is dissolved in water it dissociates to form positive ions in solution. The solution that contains these charged ions is referred to as an electrolyte. By passing sufficient amount of electric current through the electrolyte the metal cations can be reduced to deposit as solid metal. Once the template is exposed to the electrolyte and the current is applied to the conducting layer, the positively charged ions get accelerated to the bottom of the pores. When these ions reach the bottom of the pores, it interacts with the electrons that are supplied from the applied current and gets reduced to its metallic form.

This can be summed up in the following reaction:

$$M^{n+} + ne^{-} ==> M$$

The thickness of the material deposited through electroplating is dependent on the total charge. Two or more different metals can be deposited from the single electrolyte solution by using different voltages.

3.2.1 Experimental setup

The experimental setup for the electrodeposition is shown in figure 3.1. All electrochemical synthesis in this thesis was conducted potentiostatically in a standard three electrode electrochemical cell with a saturated Ag/AgCl electrode acting as reference electrode. 99.99% pure platinum mesh was used as a counter electrode. Silver was deposited on one side of the polycarbonate template which served as a working electrode.

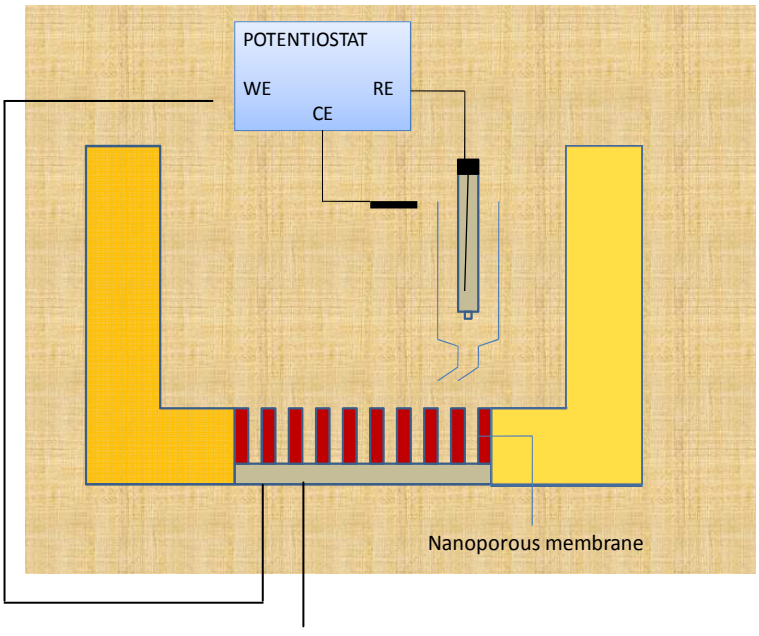

Figure 3.1 Experimental Setup

The electrochemical experiments were performed using a Princeton Applied Research Model 273A potentiostat / galvanostat with a standard-type three electrode set up connected to a Teflon electrolytic set-up. Figure 3.2 below shows the instrument used:

Figure 3.2 Potentiostat/Galvanostat Model 273A

3.2.2 Method of fabrication

Films containing multilayer segments of Au and Co were electrodeposited into the pores of commercially available ion track etched polycarbonate membranes. Each pore had a thickness of 20 micron, diameter of 100-150nm and a pore density of $2X10^8$ pores/cm^2. A 500nm conductive coating of silver was initially sputtered or evaporated on one side of the membrane to serve as a working electrode. The cell was connected and it was checked by monitoring that the voltage is not fluctuating. Multilayers of gold and cobalt were then fabricated

starting with a buffer layer. Once the deposition was done, polycarbonate template was dissolved using dichloromethane. Dichloromethane was washed away by washing the sample with water multiple times. Finally, ultrasonic was used to break all the constituents apart followed by centrifuge. A drop of this solution was spread on Au-coated silicon wafer or carbon grid and microstructural characterizations were performed using Scanning electron microscopy and Transmission electron microscopy. Magnetic characterization was done using vibrating sample magnetometer.

The following is the pictorial representation of the whole process of fabrication:

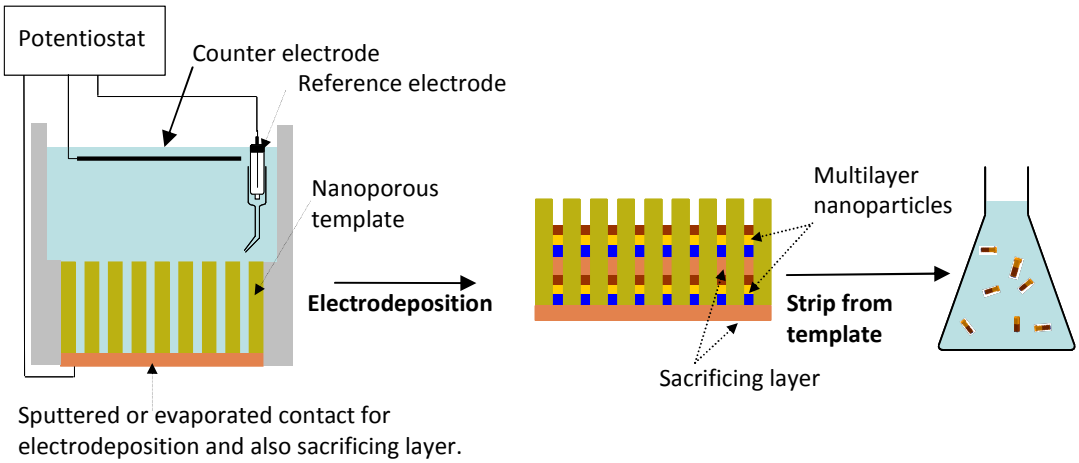

Figure 3.3 Process to fabricate multilayered nanomagnets by electrodeposition into polycarbonate template

3.3 Physical vapor deposition

Physical vapor deposition (PVD) is a general term used to describe a variety of methods to deposit thin films by condensation of a vaporized form of material onto various surfaces. The coating method involves purely physical processes such as high temperature vacuum evaporation or plasma sputter bombardment. PVD processes are commonly used for the deposition of metals.

3.3.1 Sputtering

Sputtering is a technique in which atoms are ejected from a solid target material due to bombardment by energetic ions, which then deposits on the substrate. It is driven by momentum transfer between the ions and atoms in the material which are undergoing constant collisions. As the DC power is turned on, the free electrons will immediately be accelerated away from the negatively charged cathode. These electrons encounter the outer shell electrons of the neutral gas atoms (usually Argon or Helium) in their path and will as a result eject even more electrons from them. This will ionize the neutral gas atom from Ar to Ar^+ and thus plasma is created. These positively charged Ar^+ ions are accelerated towards the cathode (target) and ejects neutral atoms, molecules and even their clusters together with some electrons. The neutral atoms are then deposited on the substrate and everywhere in the chamber and the additional electrons continue to form more ions and help in sustaining the plasma.

Magnetron sputtering

DC sputtering has proved to be a very useful technique for thin film deposition but has very low deposition rate. To overcome this problem sputtering sources usually have magnets behind, that utilize strong electric and magnetic field close to the surface of the target. The electrons follow helical paths around the magnetic field lines undergoing much more collisions with Argon atoms near the target surface than what occur in DC sputtering. The extra argon ions created as a result of these collisions leads to a higher deposition rate. Also plasma can be sustained at a lower pressure. However, the sputtered atoms are neutrally charged and so are unaffected by the magnetic trap.

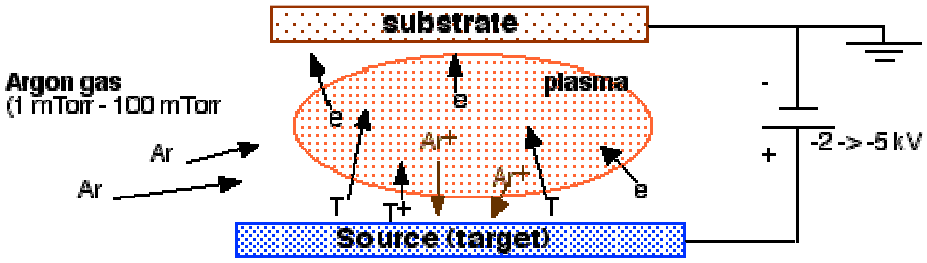

Figure 3.4 Magnetron sputtering

Following is the instrument used for the development of this thesis.

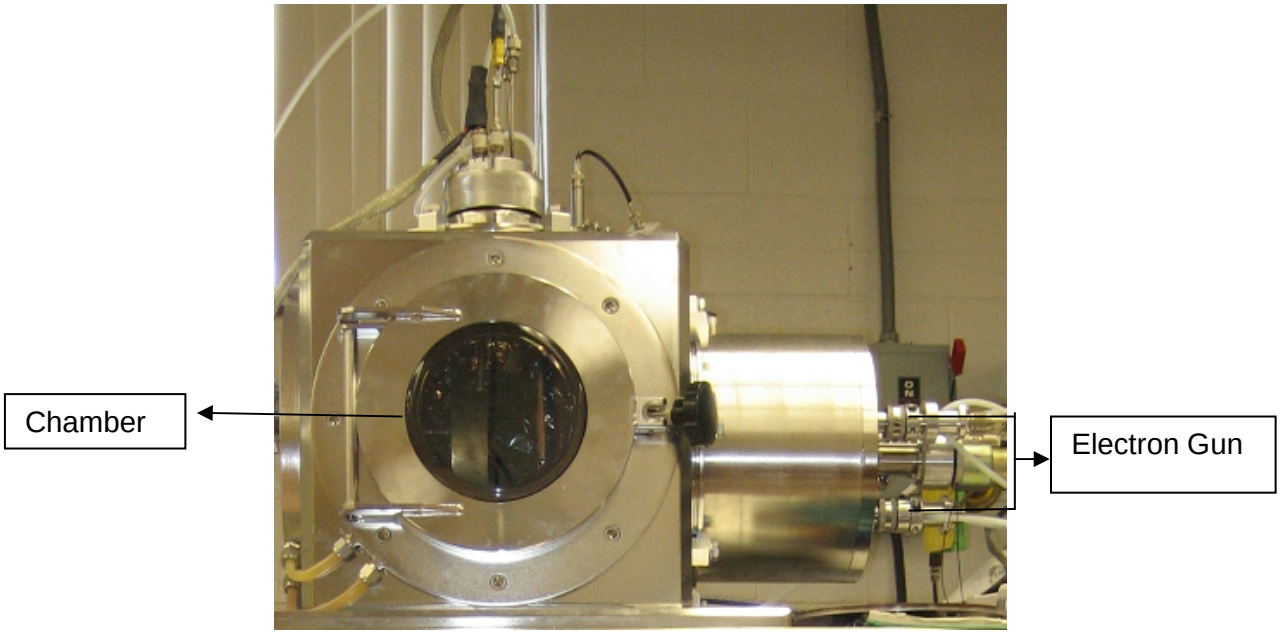

Figure 3.5 Sputtering instrument

3.4 Magnetic characterization

Magnetic characterization is carried out with instruments called magnetometer. A magnetometer is an instrument used to measure the magnetic response of samples to the

applied magnetic field. Some of the common magnetometers are Vibrating sample magnetometer and Alternating gradient magnetometer.

3.4.1 Vibrating sample magnetometer

Any magnetic specimen in a uniform magnetic field would produce a distortion of the field. A vibrating sample magnetometer is based on the flux change in a coil when a sample is vibrated near it. This is the principle of VSM.

The VSM employs an electromagnet which provides the magnetizing field (DC), a vibrating mechanism to vibrate the sample in the magnetic field, and detection coils which generate the signal voltage due to changing flux emanating from the vibrating sample. The sample is placed inside a uniform magnetic field to magnetize the sample. During the measurement, the sample is vibrated at a small frequency of around 70Hz, which produces a field distortion in an AC manner. This field distortion is detected by a pick-up coil and then is processed with conventional AC processing equipment. The sample's magnetic moment is obtained by Faraday law of induction by measuring the induced voltage across the pick-up coils according to the equation:

$$V=-N\, d\varphi/ dt$$

where N is the number of turns in the detection coils and φ is the flux in the coils, which is proportional to the magnetic moment of the sample. Figure 3.6 shows the VSM machine used:

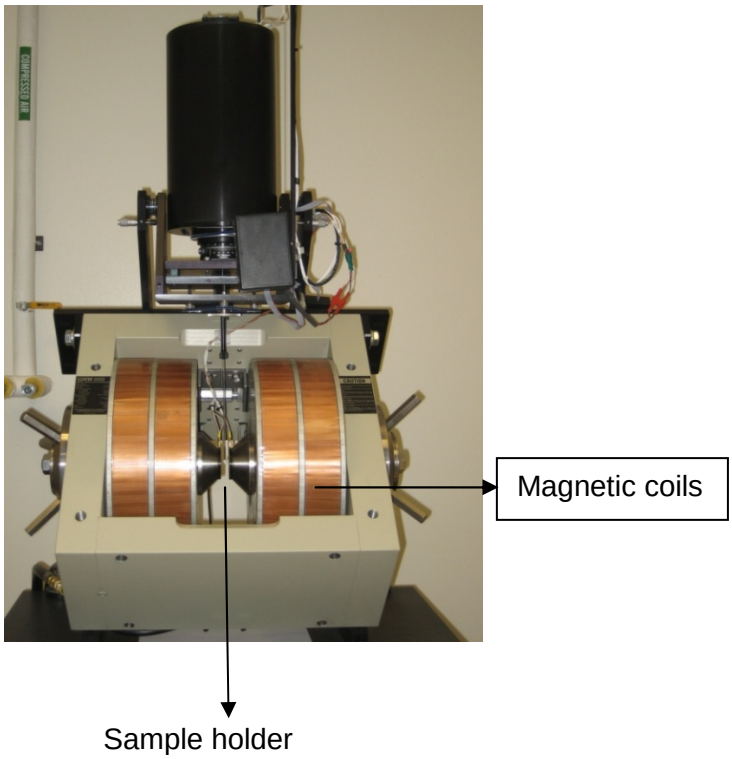

Figure 3.6 Vibrating sample magnetometer

3.4.2 Alternating gradient magnetometer

If the gradient produced by the coils in the magnetic gap is made AC instead of DC i.e. the sample is subjected to an alternating force F, the device is called Alternating Gradient Magnetometer. In AGM the sample is mounted on the tip of an extension rod (cantilever) attached to a piezoelectric element. The electromagnet produces a uniform magnetic field whereas the pair of gradient coils which are mounted to the electromagnet produces an alternating magnetic field. This means that during the measurement, the sample is magnetized by the uniform field from the electromagnet and simultaneously subjected to an alternating field

gradient, which produces an alternating force, F on the cantilever. This force is proportional to the magnitude of the gradient field, dH/dx and the magnetic moment of the sample, M:

$$F= M\, dH/dx$$

The deflection of the cantilever due to this force is proportional to the output voltage of the piezoelectric sensing element, which is synchronously detected at the operating frequency of the gradient field. Therefore the amplitude of the voltage is proportional to the sample's magnetic moment.

An AGM usually has a remarkable sensitivity of 10^{-7} emu. Generally AGM can perform a very quick measurement. But the output signal in AGM is proportional to the magnitude of the alternating field, which is an additional non-uniform field experienced by the sample. The sample with a small moment in the 10^{-6} emu range needs a higher alternating field gradient, usually of about 15 Oe/cm, to generate a sufficient signal. However, this alternating field may change the magnetization of the sample if the sample has low coercivity. AGM in general is not suitable for measuring samples with low moment and low coercivity.

Following is the AGM machine used for measurement in the thesis:

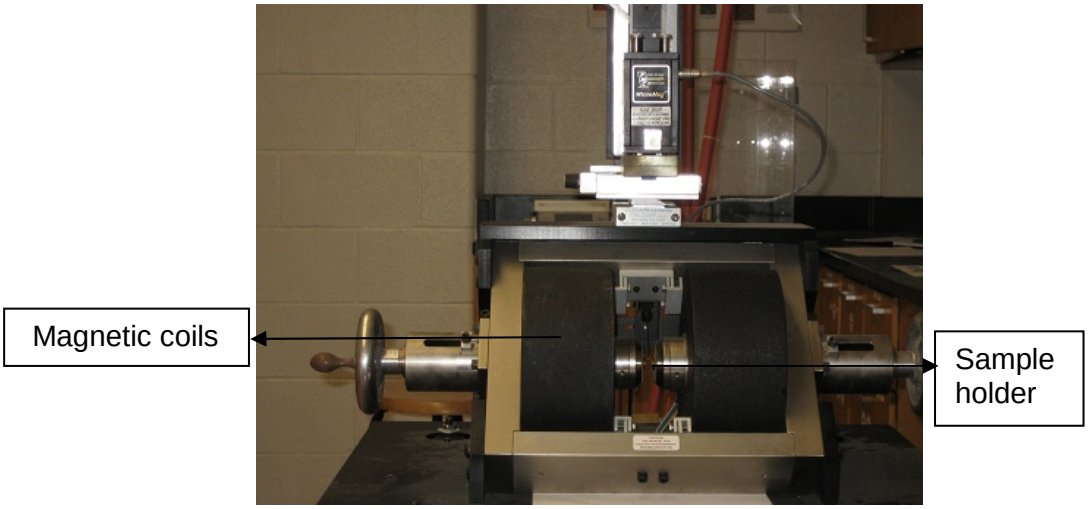

Figure 3.7 Alternating sample magnetometer

3.5. Microstructural characterization

In the present study, Scanning electron microscope and Transmission electron microscope were used for microstructural characterization.

3.5.1 Scanning electron microscope

Scanning electron microscope is a type of electron microscope that images the sample surface by scanning it with a beam of high energy electrons in a raster scan pattern. The electrons interact with atoms of the sample producing signals that contain information about the sample's surface topography, composition and several other properties. SEM produces different types of signals like secondary electrons, X-rays, backscattered electrons and light.

In a typical SEM, the electron beam is focused by one or two condenser lenses. The interaction of the electron beam and the sample results in the in the reflection of high energy electrons by elastic scattering, emission of secondary electrons by inelastic scattering and the emission of X-rays. Each of these signals are detected by a special detector.

Following is the SEM used to observe the microstructural properties of the samples

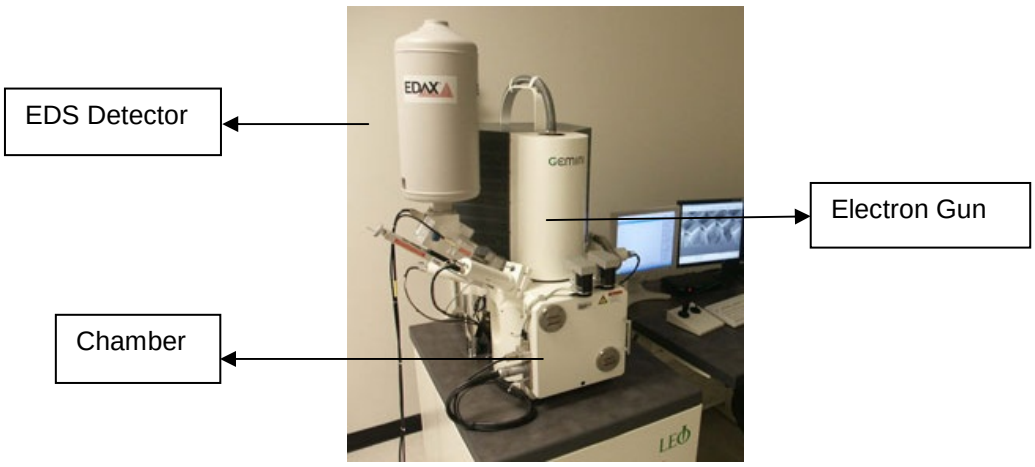

Figure 3.8 Scanning electron microscope

3.5.2 Transmission electron microscope

Transmission electron microscopy (TEM) is a microscopy technique whereby a beam of electrons is transmitted through an ultra thin specimen, interacting with the specimen as it passes through it. An image is formed from the electrons transmitted through the specimen, magnified and focused by an objective lens and appears on an imaging screen.

The transmission electron microscope (TEM) operates on the same basic principles as the light microscope but uses electrons instead of light. What you can see with a light microscope is limited by the wavelength of light. TEMs use electrons as light source and their much lower wavelength makes it possible to get a resolution a thousand times better than with a light microscope.

CHAPTER 4

RESULTS AND DISCUSSIONS

In this chapter, the experimental results will be discussed. First phase diagrams will be given to illustrate the thermodynamic equilibrium of Au and commonly used magnetic materials namely Ni, Co and Fe. Then conditions and results for the fabrication of multilayers of gold and NiFe through sputtering are demonstrated. Following that, conditions, effect of variation of parameters and method of fabrication of multilayer segments of gold and cobalt through electrodeposition are explained.

4.1 Phase diagrams

Before getting into the actual discussions of multilayers of Au and NiFe (in case of Sputtering) and Au and Co (in case of electroplating), it is important to study some of the physical and chemical properties of these materials.

Gold is a soft noble metal and has a face centered cubic structure. Its oxidation state ranges from -1 to +5, however +1 and +3 dominate. Gold melts at 1064.43°C.

Cobalt is a hard material and has a hexagonal closed packed structure. It is a ferromagnetic material. The most common oxidation states of Cobalt are 2, 3 and 4. Cobalt is required in the human body in small amounts, but at higher levels of exposure it becomes carcinogenic. The curie temperature of Cobalt is 1123°C. Curie temperature of a material is a temperature above which ferromagnetic material loses its ferromagnetic ability. This is because the thermal energy increases to an extent that the atomic moments which were parallel to each other points in random direction. Above the curie point the material becomes paramagnetic.

Nickel is a transition metal and is hard and ductile. It has FCC structure and is a ferromagnetic material. Its oxidation state ranges from 1 - 4 with 2 being the most common

state. Nickel plays various roles in biology although exposure to Nickel metal and compounds should not exceed 0.05mg/cm^3. Curie temperature of nickel is 354°C.

Iron is a transition metal and is a ferromagnetic in nature. It is BCC at low temperature and FCC at higher temperature. Its oxidation state ranges from 1-6 with 2 and 3 being the most common ones. Iron is a very essential element to nearly all organisms. Curie temperature of iron is 770°C.

NiFe alloy is called permalloy and consists of 80% Nickel and 20% iron. It has very high magnetic permeability and is used in a lot of applications as soft magnetic materials since it has a near zero magnetocrystal anisotropy.

Phase diagrams are graphs in materials science that are used to show conditions at which thermodynamically-distinct phases can occur at equilibrium. The phase diagrams of gold-cobalt, gold-nickel and gold-iron are listed in figures 4.1, 4.2 and 4.3, respectively.

A number of points are worth noting and some important properties can be obtained from these phase diagrams. For Au-Co, there are three single phase regions found on the diagram: α-Co, α-Au and liquid. α-Co is rich in Cobalt and α-Au is rich in gold. The maximum solubility of co in α-Au phase is 8.4 wt% at 997°C. The solubility limit of Au in α-Co is also around 8 wt% reaching at 1200°C. At room temperature the solid solution of α-Au and α-Co co-exist, their solubility is, however, negligible.

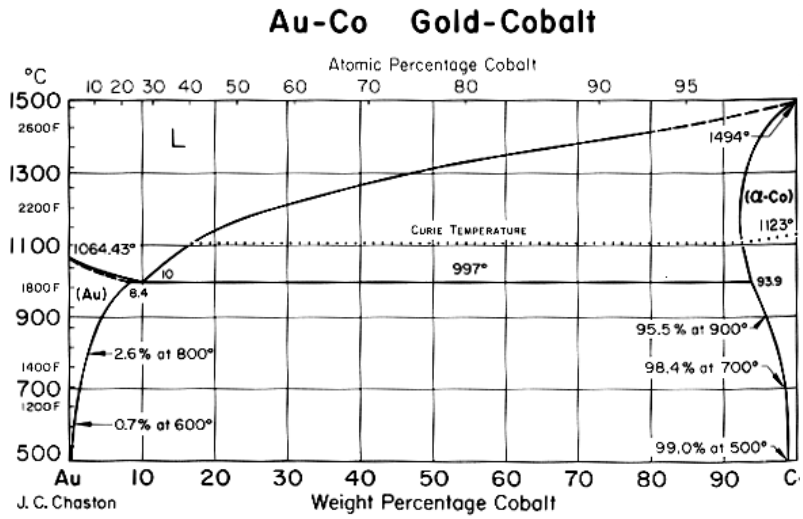

Figure 4.1 Phase diagram of gold and cobalt

In Fe-Au system, pure iron upon heating undergoes two changes in its crystal structure before melting. At room temperature, its stable form is called ferrite or α-iron and has a BCC structure. The maximum solubility of α-iron is about 3.2 wt. %. Ferrite on heating till 912°C undergoes polymeric transformation to austenite (γ-iron) which has FCC structure. Austenite persists till 1394°C and then again reverts back to BCC phase called δ-iron. δ-iron melts at 1538°C. Iron has a large solubility in Gold with maximum of 46% Fe at 1173°C at room temperature. At room temperature, solubility is still substantial and is around 2%.

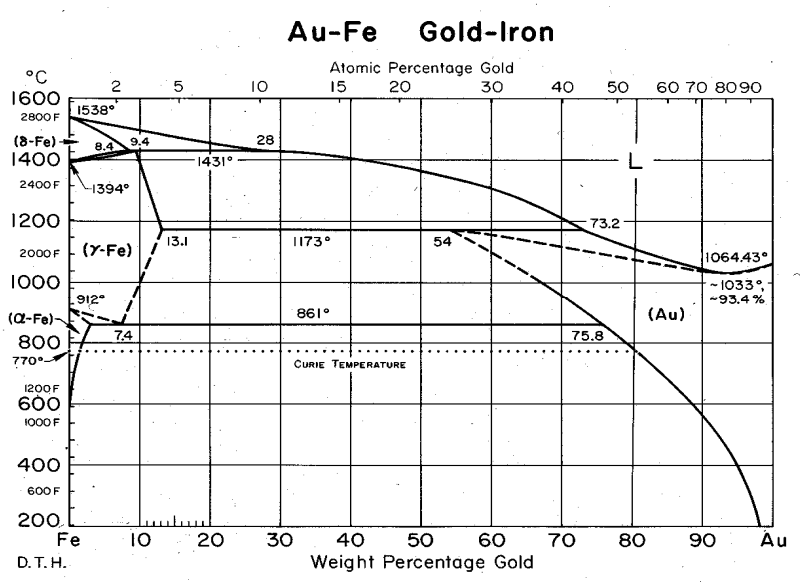

Figure 4.2 Phase diagram of gold and iron

For gold and nickel system, maximum solubility of nickel in gold is about 7 wt.% and the maximum solubility of gold in nickel is about 6 wt %. The complete solid solubility of gold and nickel happens between 821°C and 950°C when the composition of nickel is 54.4 wt %. The gap which is observed between the upper critical solution temperature (UCST) or above the lower critical solution temperature (LCST) is called miscibility gap. At room temperature the solubility is small.

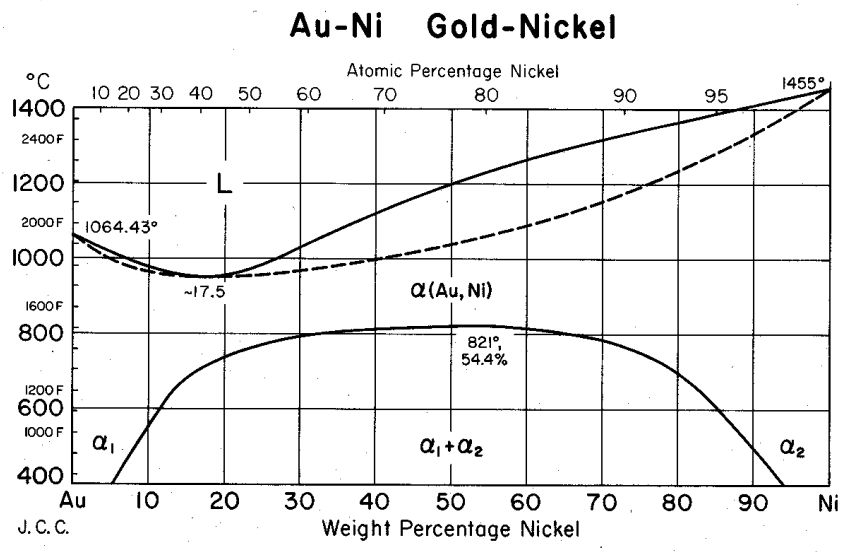

Figure 4.3 Phase diagram of gold and nickel

4.2 Fabrication of multilayers of gold and permalloy using sputtering

To prove the concept of obtaining a superparamagnetic granular film by multilayer structures, multilayers of gold and NiFe were first fabricated using sputtering. The substrate used was silicon wafer. The objective was to control the thickness of NiFe and obtain the ideal conditions for acquiring superparamagnetic films. The idea of forming such granular superparamagnetic nanoparticles can be understood from the following diagram:

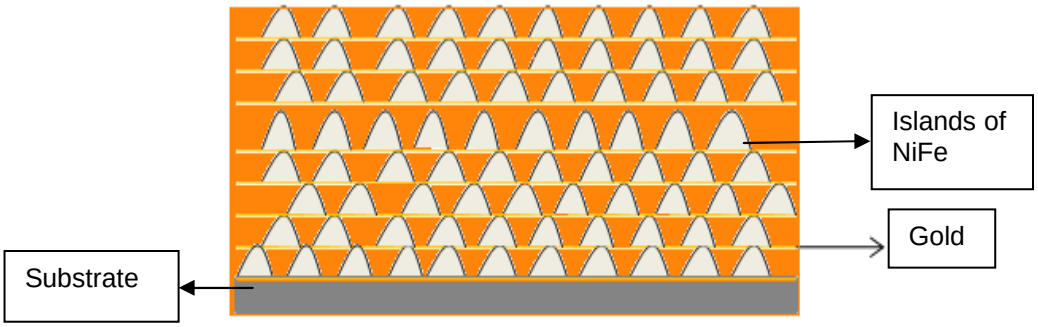

Figure 4.4 Formation of islands of magnetic material embedded in gold

The reason to choose NiFe is that it has a very small anisotropy constant. Hence large superparamagnetic particle size can be obtained which would be easier to form during sputtering. A combination of various parameters was designed and the following sets of experiments were conducted. Following table shows the materials with their sputtering rate for DC power.

Table 4.1 Sputtering specifications

	Deposition rate		
Element	80W/7.7mT	120W/7.7mT	40W/10.71mT
Gold	23.8nm/min	35.6nm/min	12.6nm/min
NiFe	8.2nm/min	12.5nm/min	3.3nm/min

40W power was used in all the experiments because it is desired to keep the deposition rate as low as possible to easily control the growth speed. This is essential for the formation of islands inside gold films. Base Pressure was maintained below $5X10^{-6}$Torr and argon pressure was kept around 7.5mTorr. Also, the multilayers will have the same gold thickness of 12.6nm

per layer. However the time of deposition for NiFe was changed systematically to obtain superparamagnetic films. Figure 4.5(a), (b) and (c) shows the hysteresis loops for these sputtered films:

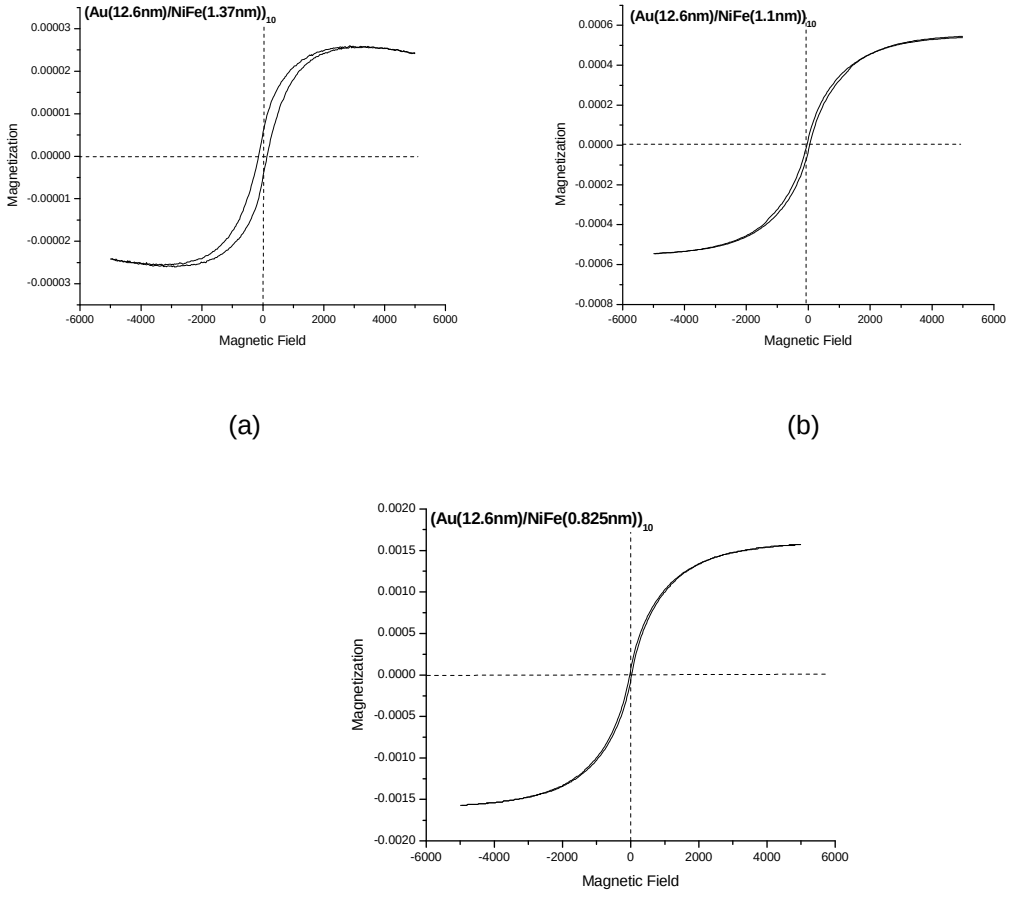

Figure 4.5 Hysteresis loop for multilayer sputtered films (a) Au (12.6nm)/NiFe(1.37nm))$_{10}$ (b) Au (12.6nm)/NiFe(1.1nm))$_{10}$ (c) Au (12.6nm)/NiFe(0.825nm))$_{10}$

The results from the above hysteresis loop are summarized in the following table:

Table 4.2 Variation of coercivity and remanance with NiFe deposition time

NiFe deposition time	Remanance(M_r/M_s)	Coercivity
25 seconds	$5.68x10^{-6}$ emu	136 Oe
20 seconds	$4.18X10^{-5}$ emu	45.5 Oe
15 seconds	$9.84X10^{-5}$ emu	11.99 Oe

From the hysteresis loops obtained and the table above it can be seen that as the thickness of NiFe decreases, coercivity and remanance also decreases. It was found that superparamagnetic film is achieved at 15 seconds of NiFe deposition.

4.3 Conditions for electrodeposition

A single-bath Au-Co solution can be prepared for the fabrication of multilayers of gold and cobalt. Cobalt sulfate hepta hydrate ($CoSO_4.7H_2O$) was used for cobalt deposition and potassium gold cyanide ($KAu(CN)_2$) was used for gold deposition. The pH was adjusted using potassium hydroxide [5]. The conditions for the preparation of single-bath electrolyte are given in the table below:

Table 4.3 Chemical composition of the Au-Co electrolyte

Chemical used	Molecular Formula	Composition
Cobalt Sulfate Hepta Hydrate	$CoSO_4.7H_2O$	0.285M
Citric Acid	$C_6H_8O_7$	0.8M
Potassium Gold Cyanide	K $Au(CN)_2$	$3X10^{-4}$M

The concentration of gold is approximately $3X10^{-4}$M while the concentration of cobalt is 0.285M. It is obvious that when cobalt is deposited at -1V, some gold is also deposited because the reduction potential of Gold (+1.50V) in aqueous solution at 25°C is more positive than cobalt

(-0.28V). But because the concentration of Gold is very less as compared to Cobalt, the amount of gold deposition is really small at -1V. Hence the formation of an alloy of Gold and Cobalt is negligible. On the other hand while depositing gold, cobalt does not get deposited because reduction potential of Cobalt is more negative than gold. Following are the reduction potential of gold and cobalt at 298K, 1 M and 1 atm.

Half Reaction	E^o(V)
$Au^{3+}_{(aq)} + 3e^- \longrightarrow Au_{(s)}$	+1.50
$Co^{2+}_{(aq)} + 2e^- \longrightarrow Co_{(s)}$	-0.28

This is why a single bath can be used for Au and Co deposition which makes the entire process simple and free of contamination.

It will be observed later that copper will be used as a buffer layer in the fabrication of multilayers. The process then becomes double bath. Copper sulfate heptahydrate was used to prepare the electrolyte which is used for depositing copper as a buffer layer. The composition used is as follows:

Table 4.4 Chemical composition of the copper deposition electrolyte

Chemical used	Molecular Formula	Composition
Copper Sulfate Hepta Hydrate	$CuSO_4.7H_2O$	0.5M
Sulfuric Acid	H_2SO_4	1mL

4.4 Electrodeposition: Effect of various parameters on fabrication process

Before the fabrication of multilayer films of gold and cobalt inside the template, it is important to study the effect of various parameters which can vary the electrodeposition process. The electrodeposition of cobalt can be characterized by measuring magnetic properties of deposited films. The effect of pH, concentration of Gold and the voltage applied on cobalt deposition were studied. For comparison, all samples were cut into the same area and

their hysteresis loops were measured. All these experiments were performed on a gold coated silicon wafer.

4.4.1 Effect of pH on deposition rate of cobalt

For the deposition of multilayer of gold and cobalt, controlling the pH value is crucial. A variation of pH was studied to find out the effect it has on the deposition of Cobalt. This was done by keeping all the parameters the same, except the pH of the solution.

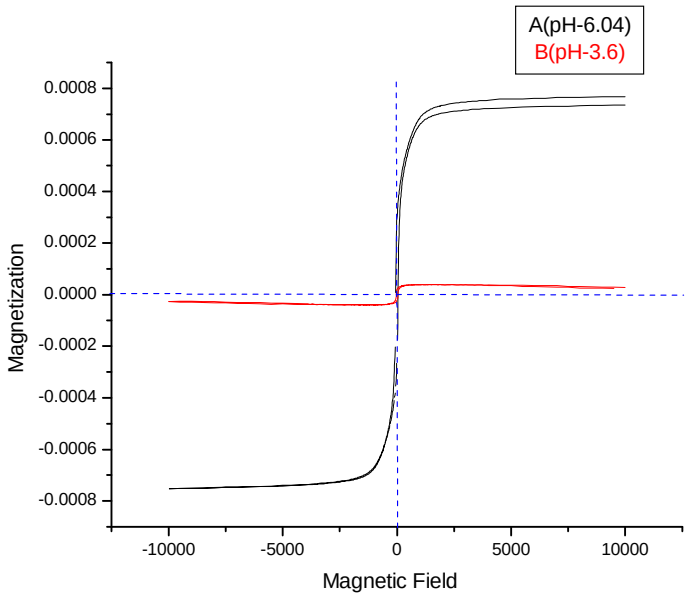

Figure 4.6 Effect of pH on cobalt deposition rate

The results obtained from the above VSM graph can be summarized in the table below:

Table 4.5 Variation of magnetic moment, remanance and coercivity with pH

pH	Co con.	Au Con.	Time	Moment	Remanance	Coercivity
3.61	0.285M	$3X10^{-4}$ M	1000 sec	$4X10^{-5}$ emu	$1.88X10^{-5}$ emu	30.2 Oe
6.04	0.285M	$3X10^{-4}$ M	1000 sec	$8X10^{-4}$ emu	$2.87X10^{-4}$ emu	60.1 Oe

It can be seen that the moment of the sample with pH of 6.04 is $4X10^{-5}$ emu and it reduces by more than 10 times on decreasing the pH to 3.5. Hence, it can be concluded that as pH increases, cobalt deposition and hence moment also increases. However, pH was maintained between 3.5 and 4 for all the experiments. This is because it was observed that as the pH is increased there is a sharp decrease in gold deposition. This defeats the purpose of making these particles because gold is what makes these nanoparticles biocompatible and functionalizable for biomolecule attachment.

4.4.2 Effect of gold concentration on cobalt film formation

It was also found that if the concentration of Gold is increased beyond $3X10^{-4}$M, the moment sharply increases. Following two samples show the change in moment with gold concentration.

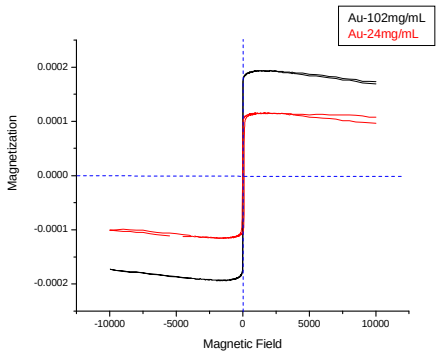

Figure 4.7 Effect of gold concentration on cobalt deposition rate

The results from the above hysteresis loop can be summarized in the table below:

Table 4.6 Variation of magnetic moment, remanance and coercivity with Au concentration

pH	Co Con.	Au Con.	Time	Moment	Remanance	Coercivity
3.65	0.285M	$5.17X10^{-3}$M	200 sec	$1.2x10^{-4}$emu	$1.57X10^{-4}$ emu	28.31 Oe
3.65	0.285M	$3X10^{-4}$M	200 sec	$2x10^{-4}$ emu	$9.32X10^{-5}$ emu	14.99 Oe

An important point to be considered here is that the moment increases on increasing the gold concentration which is actually desired. This is because larger the moment, easier it would be to direct the nanoparticle more precisely to the affected organ. However, there is a limitation. It has been discussed that Cobalt is deposited at a potential of -1V and gold at -0.49V. So while depositing cobalt, small amount of gold is also getting deposited. This leads to the formation of a gold-cobalt alloy which is undesirable. Hence if the amount of gold is increased beyond the threshold of $3X10^{-4}M$ then the chances of formation of a Au-Co alloy becomes very high. Therefore, a balance has to be maintained between the gold concentration and the moment desired.

4.5 Fabrication process of multilayers of gold and cobalt

In this thesis, multilayer of gold and cobalt were fabricated inside polycarbonate track etched membrane (20micron length and 100nm diameter). In the experimentation 5 methods of fabrication were attempted:

- Bulk Film Magnetic Properties
- Multilayer deposition inside the template
- Multilayer deposition with gold as a buffer layer.
- Multilayer deposition with cobalt as a buffer layer.
- Multilayer deposition with copper as buffer layer

Bulk film properties were measured by depositing multilayers of gold and cobalt on a silver coated silicon wafer. The purpose of depositing a bulk film on the wafer was to ensure if we can really deposit Au and Co using Au/Co electrolyte at the voltages found out from cyclic voltammetry (-0.49V for Gold and -1V for Cobalt). Another purpose was to find out the conditions for superparamagnetism.

4.5.1 Bulk film properties

A bulk film sample is fabricated with Au/Co single-bath electrolyte with cobalt deposition at -1V and gold deposition -0.49V. 10 layers of 1000seconds of Au and 40sec of cobalt were deposited.

On measuring the magnetic properties of the sample following hysteresis loop was obtained:

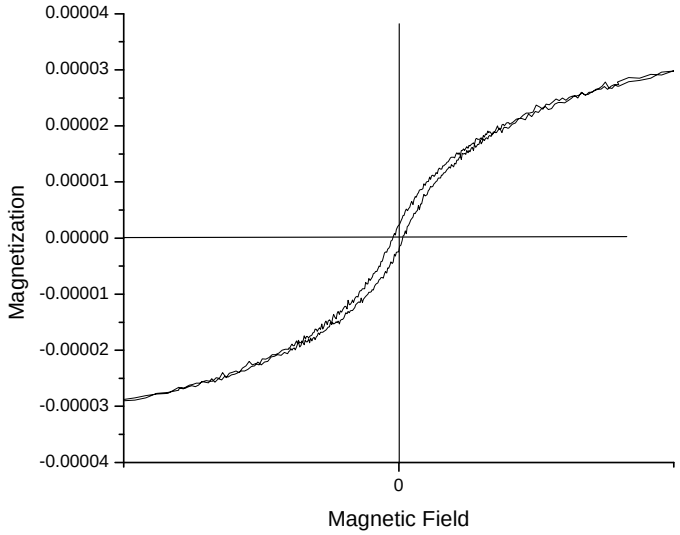

Figure 4.8 Bulk film magnetic properties

Since cobalt is deposited for a total of 400 seconds in 10 layers and hence the magnetic property of this sample is ferromagnetic. It clearly shows that using these deposition conditions, multilayer of Au/Co can be obtained.

4.5.2 Multilayer deposition inside the template

First, a long segment of gold was deposited followed by a long segment of cobalt inside the template. Following micrograph was obtained from SEM:

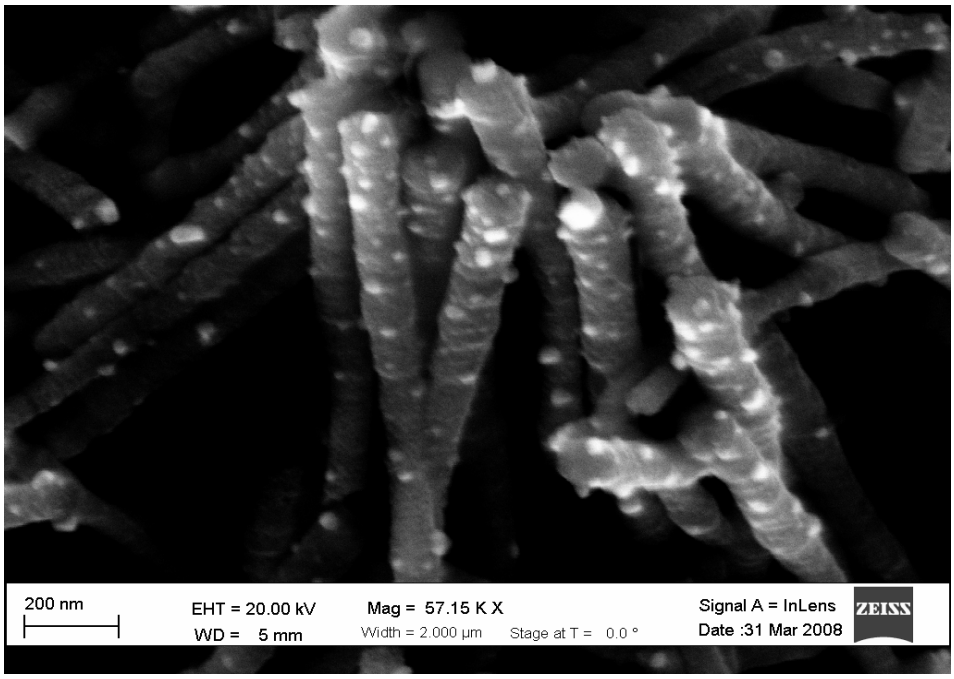

Figure 4.9 Deposition of gold and cobalt inside template

It can be clearly seen from the micrograph that gold is deposited on the wall of polycarbonate membrane. This may happen because silver which is sputtered or evaporated on the back side of the template also grows on the wall. Hence, gold instead of depositing inside the template deposits on the wall. It can be seen that in depositing the multilayer it is necessary to have a buffer layer. Also, the buffer layer needs to be long enough to cover the electrode on the inner wall surface. Deposition of 1000 seconds of gold is not sufficient to serve as a buffer layer.

4.5.3 Multilayer deposition with gold as a buffer layer

After noticing the results of a sample with no sacrificial layer in the previous section, a longer segment of gold was deposited as a buffer layer. 2000seconds of gold was deposited as

a buffer layer followed by 4 layers of 700 seconds of gold and 25seconds of cobalt. The magnetic properties of the sample can be observed as follows:

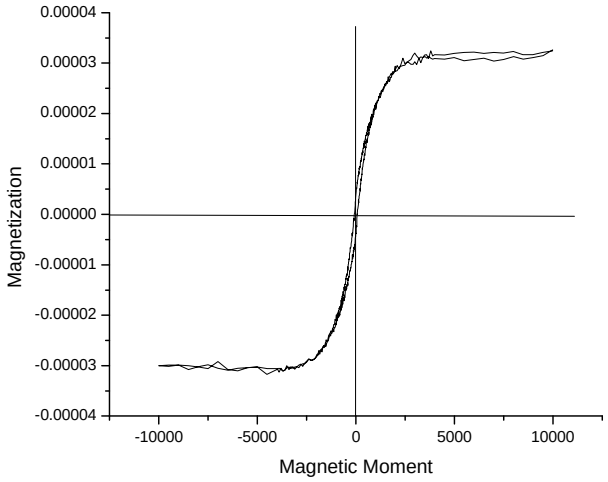

Figure 4.10 VSM for multilayer deposition of gold and cobalt with gold as a buffer layer.

Scanning electron microscope was done to obtain micrographs of the multilayers.

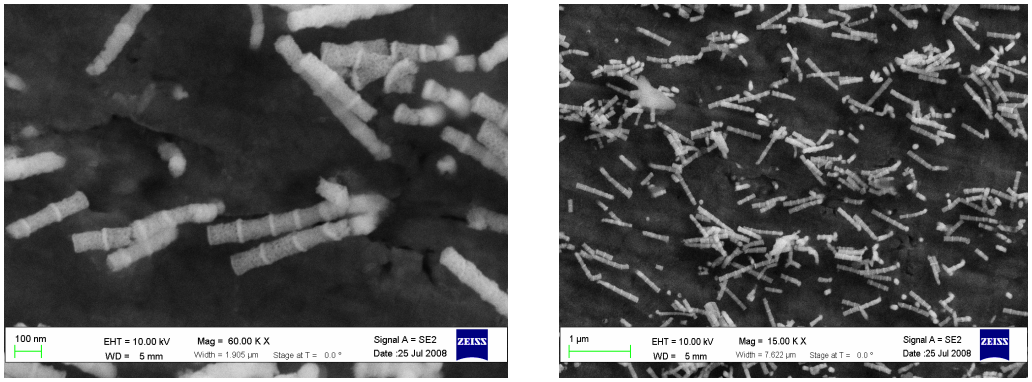

Figure 4.11 Multilayer deposition of gold and cobalt with gold as a buffer layer

The multilayer of gold and cobalt can be clearly seen in the above micrograph. The contrast in the picture indicates the two materials. Gold is brighter because of its higher atomic number and Cobalt is darker.

Transmission Electron Microscopy (TEM) was also done for this sample to observe the microstructural characteristics for the sample above. For TEM, the particles were dissolved in solution. After dissolving polycarbonate template using dichloromethane the sample was then washed away with water multiple times. Then ultrasonic was done to break all the constituents apart followed by centrifuge to settle down all the particles. After centrifugation, a drop was taken from the solution at the bottom to view a TEM image. The image obtained is as follows:

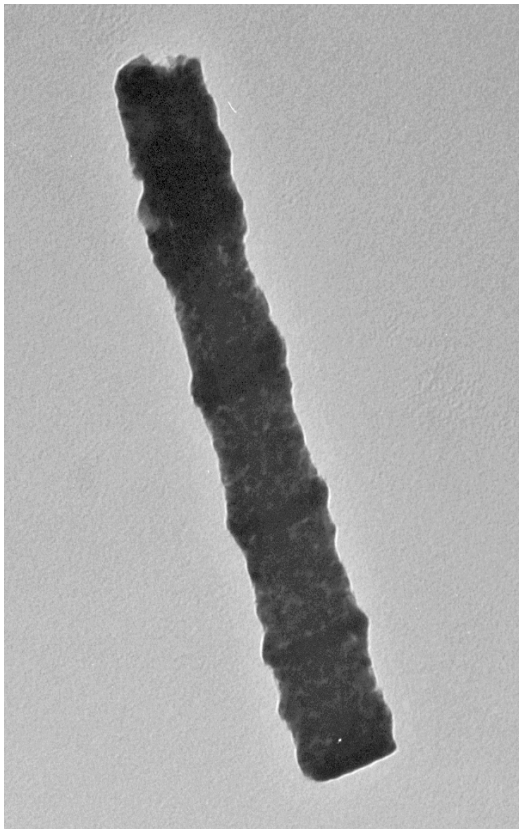

Figure 4.12 TEM for multilayer deposition of gold and cobalt with gold as a buffer layer

4.5.4 Multilayer deposition with cobalt as a buffer layer

Next Cobalt was deposited as a sacrificial layer. As mentioned, a sacrificial layer is used to form the whole structure of multilayers but is eventually dissolved and is not a part of the final structure. In this case, three sets of multilayer were deposited seperated by a long segment of Cobalt as a sacrificial layer. 3 cycles of 5 layers of 500 seconds of Au and 25 seconds of Cobalt were deposited. The 3 sets of multilayers can be clearly observed between the three long segments of Cobalt in the SEM micrograph:

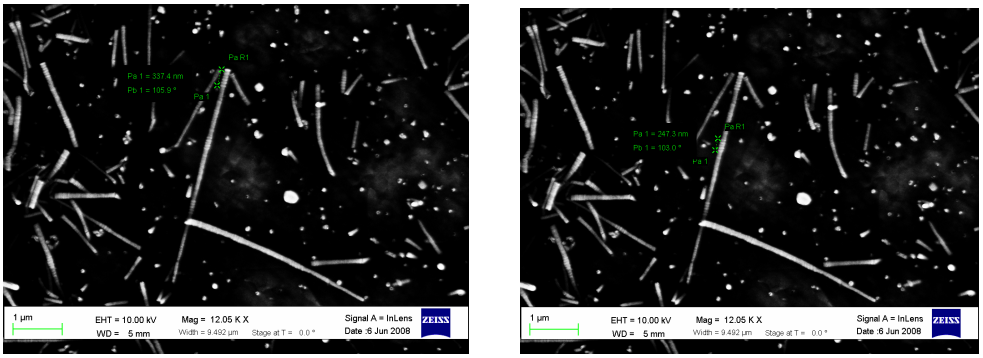

Figure 4.13 Multilayer deposition of gold and cobalt with cobalt as a buffer layer

The total length of the multilayers is 337.4nm.and the long segment of Cobalt is more than 1 micron long. The magnetic property of this sample will always be ferromagnetic because of the long segment of cobalt being used as a sacrificial layer. The VSM for this sample is as follows:

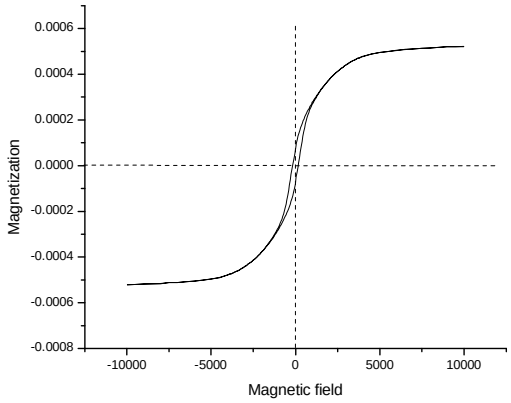

Figure 4.14 VSM for multilayer deposition of gold and cobalt with cobalt as a buffer layer

4.5.5 Multilayer deposition of Au/Co with copper as a buffer layer

A very clear SEM micrograph of multilayers was obtained when cobalt was used as a buffer layer. But, to study the magnetic properties of multilayers, Co cannot be used since it provide strong magnetic signal. Hence a different sacrificial layer like Copper has to be deposited so that the magnetic property can be measured. However, the drawback of this method is that it is a double bath process- one bath for Au/Co deposition and the other for copper deposition. The double bath process causes more complexity, is time consuming and might cause contamination as the template is exposed to the environment.

Before the multilayer deposition a long segment of copper is deposited as a buffer layer. 1500 seconds of Copper was deposited as a sacrificial layer. Then 36 layers of 700sec of gold and 20seconds of cobalt were deposited. Following VSM graph was obtained:

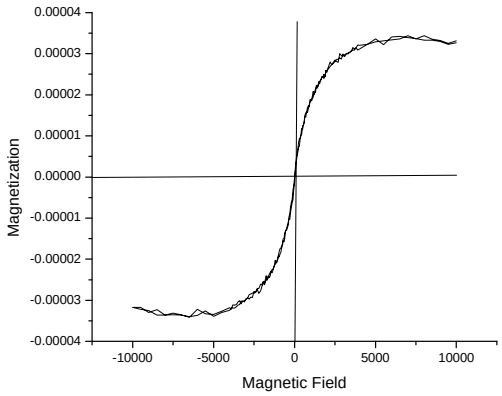

Figure 4.15 VSM for multilayer deposition of gold and cobalt with copper as a buffer layer

It can be observed that the remanance and coercivity of the sample is very small and hence it can be concluded that the particles are superparamagnetic. To confirm the superparamagnetic property, measurement was also done with using SQUID magnetometer.

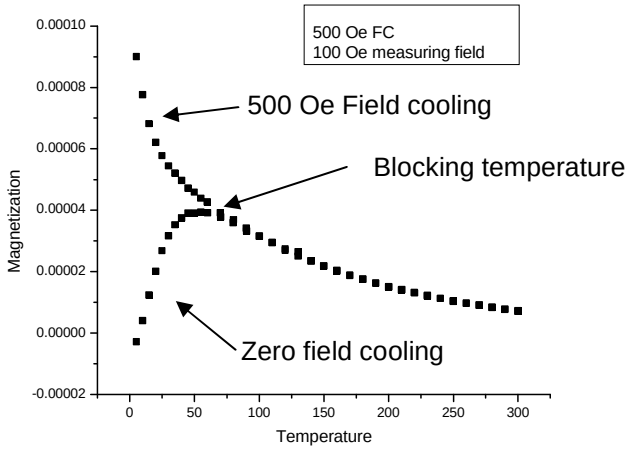

Figure 4.16 SQUID measurement for multilayer deposition with copper as a buffer layer

This is a low temperature measurement from Superconducting quantum interference devices (SQUID). There were two types of cooling mechanisms- Field cooling with an applied

field of 500 Oe and zero field cooling. In the field cooling mechanism, a 500 Oe of field was applied to align the atomic moments in the direction of the field. The measurement was done at 100Oe. Here in contrast to AGM or VSM, 500 Oe of field is enough to align the moments because at a temperature of 5K the thermal energy is very less. Now on increasing the temperature through 5K till 300K, thermal energy increases and the atomic moments starts to point in random directions thus reducing the magnetic moment [25]. The zero-field cooling mechanism is used in which no field is applied. In this case the 100Oe field applied to measure the magnetic moment which is not sufficient to align the atomic moments in the same direction. Hence at 5K the magnetic moment is very low. Now as the temperature is increased the thermal energy increases and hence the atomic moments starts to change directions and randomize. At a particular temperature (around 50K in this case) the particles become superparamagnetic. This temperature is called blocking temperature. Above this blocking temperature the particles are superparamagnetic and below it, the particles are ferromagnetic.

The SEM result of such a sample shows the color contrast between the long sacrificial layer of copper and multilayer of gold and cobalt. In the SEM graph the dark long segment seen is the Copper sacrificial layer and the bright top peak is like cobalt embedded in gold.

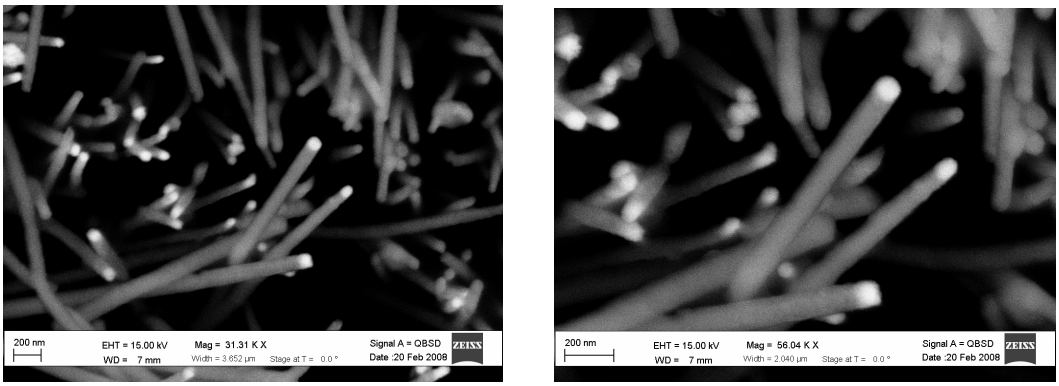

Figure 4.17 Multilayer deposition with copper as a buffer layer

It is clearly observed that when copper is used as a buffer layer, multilayers cannot be seen. The buffer layer completely changes the deposition process. The reason for this drastic change is currently being investigated.

CHAPTER 5

CONCLUSIONS

A preliminary study was conducted and conditions were identified to produce superparamagnetic property in the multilayer of Au and Co using single-bath electrodeposition. samples. Several conclusions can be drawn from this study:

1) Desirable pH for deposition of multilayer of Gold and Cobalt is between 3.5 and 4.

2) Gold concentration in the electrolyte should be around $3X10^{-4}M$ otherwise the chances of gold and cobalt alloy formation become high.

3) The solution has to be changed every 3-4 layers so as to deposit enough gold.

4) Suitable voltage required for Au deposition is -0.49V and Co deposition is -1V above which hydrogen evolution takes place.

5) A sufficiently long sacrificial layer has to be deposited in order to see the multilayers. Otherwise gold just deposits on the wall of polycarbonate.

6) Clear multilayer can be observed when gold and cobalt are used as sacrificial layer. But when copper is used as a sacrificial layer, only cobalt embedded in gold can be seen, which becomes superparamagnetic.

REFERENCES

1) Pedro Tartaj, Maria del Puerto Morales, Sabino Veintemillas-Verdaguer, Teresita, Gonzales-Carreno and Carlos J Serna, The Preparation of magnetic nanoparticles for applications in biomedicine, J. Applied Physics 36,(2003), R182-R 197.

2) Q A Pankhurst, J Connolly, S K Jones and J Dobson, Applications of magnetic nanoparticles in biomedicine, Journal of Applied Physics,36, (2003), R167-R181.

3) Stephane Mornet, Sebastien Vasseur, Fabien Grasset and Etienne Duguet, Magnetic nanoparticle design for medical diagnosis and therapy, Journal of Materials Chemistry,14,(2004), 2161-2175.

4) John C. Hulteen and Charles R. Martin, A general template based method for preparationof nanomaterials, Journal of Materials Chemistry, 7(7), 1997, 1075-1087.

5) Sima Valizadeh, Lars Hultman, Jean-Marie George and Peter Leisner, Template Synthesis of Au/Co Multilayered Nanowires by Electrochemical Deposition, Adv. Funct. Materials, 12,(2002),11-12.

6) Catherine C Berry and Adam S G Curtis, Functionalisation of magnetic nanoparticles for applications in biomedicine, Journal of Applied Physics, 36,(2003), R198-R206

7) Ju Hun Lee, Jun Hua Wu, Hong Ling Liu, Ji Ung Cho, Moon Kyu Cho, Boo Hyun An, Ji Hyun Min, Su Jung Noh and Young Keun Kim, Iron- Gold Barcode Nanowires, Angew. Chem. Int. Ed., 46, (2007), 3663-3667.

8) A. Dolati, MGhorbani,M.R. Ahmadi, An electrochemical study of Au-Ni alloy electrodeposition from cyanide-citrate electrolytes, Journal of Electrochemical Chemistry 577,(2005), 1-8.

9) Andreas Jordon, Regina Scholz, Peter Wust, Horst Fahling, Roland Felix, Magnetic Fluid Hyperthermia(MFH): Cancer treatment with AC magnetic field induced excitation of biocompatible Superparamagnetic nanoparticles, Journal of Magnetism and magnetic materials, 201 (1999), 413-419.

10) R.E. Rosensweig, Heating magnetic fluid with alternating magnetic field, Journal of Magnetism and Magnetic Materials, 252 (2002),370-374

11) Xu Wang and Cengiz S. Ozkan, Multisegment Nanowires Sensors for the detection of DNA Molecules, American Chemical Society, (2007), A-G.

12) Prashant K. Jain, Ivan H. El-Sayed and Mostafa A, El Sayed, Au Nanoparticles target cancer, 2, (2007)

13) Ivo Safarik and Mirka Safarikova, Magnetic Nanoparticles and Biosciences, Chemical Monthly,133 (2002),737-759

14) Abhilash Sugunan and Joydeep Dutta, Nanoparticles for Nanotechnology, Journal of Physics Science and Idea,4 (2004), No. 1 &2

15) Lingyan Wang, Hye- young Park,Stephanie I-Im Lim, Mark J. Schadt, Derrick Mott, Jin Luo, Xin Wang and Chuan-Jian Zhong, Core@shell nanomaterials: gold-coated magnetic oxide nanoparticles, Journal of Materials Chemistry, 18 (2008),2629-2635

16) Anand Gole, John W. Stone, William R. Gemmill, Hans-conrad zur Loye and Catherine J Murphy, Iron Oxide Coated Gold Nanorods: Synthesis, Characterization and Magnetic Manipulation, American Chemical Society, 24 (2008), 6232-6237.

17) P. de. La Presa, M. multigner, M.P. Morales, T. rueda, E. Fernandez-Pinel, A. Hernando, Synthesis and characterization of FePt/Au- core-shell nanoparticles,Journal of Magnetism and Magnetic Materials, 316, (2007), e753-e755

18) Marie-Christine Daniel and Didier Astruc, Gold Nanoparticles: Assembly , Supramolecular Chemistry, Quantum-Size-Related Properties and applications toward Biology, Catalysis and Nanotechnology, American Chemical Society, 104 (2004), 293-346.

19) Kyoungia Woo, Jangwon Hong, Sungmoon Choi, Hae-Weon Lee, Jae-Pyoung Ahn, Chul Sung Kim and Sang Won Lee, Easy Synthesis and Magnetic Properties of Iron Oxide Nanoparticles, American Chemical Society, 16 (2004), 2814-2818.

20) M.A. Willard, L.K. Kurihara, E.E. Carpenter, S. Calvin and V.G. Harris, Chemically prepared magnetic nanoparticles, International Materials Review, 49 (2004), 125-144.

21) D. H. Reich, M. Tanase, and A. Hultgren, L. A. Bauer, C. S. Chen, G. J. Meyer, Biological applications of multifunctional magnetic nanowires, Journal of applied Physics, 93 (2003), 7275-7280.

22) Zachary G. Forbes, Benjamin B. Yellen, Kenneth A. Barbee, and Gary Friedman, An Approach to Targeted Drug Delivery Based on Uniform Magnetic Fields, IEEE transactions on Magnetics, 39 (2003) 3372-3377.

23) Ramazan Asmatulu, Michael A. Zalich, Richard. O. Claus, Judy S. Riffle, Synthesis, characterization and targeting of biodegradable magnetic nanocomposite particles by external magnetic fields, Journal of Magnetism and Magnetic Materials 292 (2005) 108–119

24) Y. R. Chemla, H. L. Grossman, Y. Poon, R. McDermott, R. Stevens, M. D. Alper, and J. Clarke, Ultrasensitive magnetic biosensor for homogeneous immunoassay, 97 (2000) 14268-14272.

25) Manuel Arruebo, Rodrigo Fernández-Pacheco, M. Ricardo Ibarra, and Jesús Santamaría, Magnetic nanoparticles for drug delivery, 2 (2007) 22-32.

26) Rudolf Hergt, Silvio Dutz, Robert M¨uller and Matthias Zeisberger, Magnetic particle hyperthermia: nanoparticle magnetism and materials development for cancer therapy, Journal of Physics, 18 (2006) S2919-S2934.

27) S. Mornet, S. Vasseur, F. Grasset, P. Veverka, G.Goglio, A.Demourgues, J. Portier, E. Pollert, E.Duguet, Magnetic nanoparticle design for medical applications, Science Direct, 34 (2006) 237-247

28) Ajay Kumar Gupta, Mona Gupta, Synthesis and surface engineering of iron oxide nanoparticles for biomedical applications, Science Direct, 26(2005) 3995-4021

29) Young-wook Jun, Jin-sil Choi and Jinwoo Cheon, Heterostructured magnetic nanoparticles: their versatility and high performance capabilities, Chemistry communication, (2007) 1203-1214

30) Akira Ito,1 Masashige Shinkai,2 Hiroyuki Honda,1 and Takeshi Kobayashi, Medical Application of Functionalized Magnetic Nanoparticles, Journal of Bioscience and Bioengineering, 100 (2005)1-11

BIOGRAPHICAL INFORMATION

Mr. Rishi Wadhwa was born in New Delhi, India on 16 January, 1984. He got his primary education from Cambridge High School, New Delhi. He earned his Bachelor of Technology degree in Information Technology from Guru Gobind Singh Indraprastha University, India in 2005. In fall 2006, he joined University of Texas at Arlington in the Material Science and Engineering department to pursue a Master of Science degree. Currently, he is a candidate for the degree of Master of Science in Material Science and Engineering to be awarded in December, 2008.